Energy Reports 8 (2022) 1091–1113

Contents lists available at ScienceDirect

Energy Reports

journal homepage: www.elsevier.com/locate/egyr

Review article

Review on classification of resonant converters for electric vehicle application

Sheetal Deshmukh (Gore) [a,*], Atif Iqbal [a], Shirazul Islam [a], Irfan Khan [b], Mousa Marzband [c,d], Syed Rahman [b], Abdullah M.A.B. Al-Wahedi [e]

[a] Department of Electrical Engineering, Qatar University, Qatar
[b] Clean and Resilient Energy Systems (CARES) Lab, Texas A&M University, Galveston TX 77553, USA
[c] Northumbria University, Electrical Power and Control Systems Research Group, Ellison Place NE1 8ST, Newcastle, upon Tyne, United Kingdom
[d] Center of Research Excellence in Renewable Energy and Power Systems, King Abdulaziz University, Jeddah 21589, Saudi Arabia
[e] KAHRAMAA, Doha, Qatar

ARTICLE INFO

Article history:
Received 29 September 2021
Received in revised form 22 November 2021
Accepted 6 December 2021
Available online xxxx

Keywords:
Electric vehicle
Resonant converter
LLC
CLLC converter
Resonant tank circuit

ABSTRACT

The conventional hard-switching converters suffer from the limitations like the upper limit on switching frequency, high electromagnetic interference (EMI), more switching losses, large size, increased weight and low efficiency. To overcome these limitations, resonant converters are popularly used in chargers of electric vehicles (EVs). However, the detailed classification of resonant converters used in EVs is not sufficiently discussed in the literature. The guideline to select a resonant converter based topology required to charge an EV on the basis of its rating is not mentioned. To fill this gap, this paper presents a state-of-art literature survey of various resonant converter based topologies used in chargers of EVs. This paper focuses on a detailed classification of resonant converters used in the second stage of EV chargers. Further, it provides a guideline to designers to choose a converter topology used in the first stage and the second stage of EV charger required based on wattage, unidirectional and bidirectional power flow. Depending on the number of reactive elements present in a given resonant converter topology, these are classified as two-element, three-element, and multi-element resonant converters. Depending upon the connection of inductive (L) and capacitive (C) elements with respect to transformer winding, these converter topologies are further categorized as series, parallel (two-elements), inductor–inductor–capacitor (LLC) (three-element) and capacitor–inductor–inductor–capacitor (CLLC) (Multi-elements). However, the LLC type resonant converters offer high efficiency, zero-voltage switching (ZVS turn-on, turn-off) and low voltage stress on switches and high power density. Therefore, this paper mainly focuses on LLC type resonant converter topology. In addition, various modulation schemes and control schemes for LLC, CLLC resonant converter along with control of active power and reactive power are discussed for vehicle-2-grid (V2G) mode of operation.

Contents

* Corresponding author.
E-mail address: sd1912817@student.qu.edu.qa (S. Deshmukh (Gore)).

https://doi.org/10.1016/j.egyr.2021.12.013

1. Introduction

Electric vehicles (EVs) are becoming extensively popular. Due to the rapid depletion in fossil fuels, emission of greenhouse gas (GHG) and fuel cost. It is estimated by the Stated Policies Scenario that EV stock will be around 8 million by 2019 and is expected to expand up to 50 million by 2025. In the same sequence, EV penetration will grow up to 140 million by 2030. The total contribution of electric vehicles by 2030 would be approximately 7% of the total vehicles in operation (Bae et al., 2021; Liu, 2020; Jing et al., 2018).

Chargers are required to charge the battery which is included in the EV. These EV chargers are classified into five categories which are listed in Table 1 (Li et al., 2019; Kisacikoglu et al., 2012). Depending upon the converter topology, the EV charger are classified as dedicated and integrated types of EV chargers. In the case of a dedicated charger, a separate charger is provided to charge the battery, while in the case of an integrated charger, an existing propulsion equipment is used to charge the battery (Metwly et al., 2020). Depending upon the mounting of EV chargers these are classified as on-board and off-board. In the case of an on-board charger, the charging converter is mounted inside the vehicle, while in the case of an off-board charger the charging converter is mounted outside the EV. Off-board chargers are fast chargers as compared to on-board chargers (Valente et al., 2021). Depending upon the connection of EV to the charging station, EV chargers are classified as inductive, conductive. In the case of inductive charging technique, an electromagnetic field is used to transfer power from a transmitter coil to a receiver coil. Transmitter coil is connected to the charging utility, while the receiver coil is mounted on EV. In case of inductive charging magnetic field is responsible for transferring the energy from the transmitter coil to receiver coil. However, in the case of capacitive charging technique, this energy can be transferred from transmitter coil to receiver coil with the help of an electric field. In case of conductive charging technique, the energy required for charging the battery is transferred by the utility or main grid to the EV with the help of an inter-connecting cable or wire. Depending upon the output, of EV chargers these are classified as AC and DC chargers. Further, depending upon the direction of power flow EV chargers are classified as unidirectional and bidirectional chargers. If the energy can be transferred only in one direction i.e. from grid to EV (G2V) is called as unidirectional charger. If the energy can be transferred from grid to EV and EV to main grid (V2G), it is called as bidirectional EV charger. The bidirectional charger are further classified as single-stage and two-stage chargers. In the case of a single-stage charger there is no DC-link capacitor only an isolated AC/DC converter is present. On the other hand the two-stage has a DC-link capacitor that is huge in size and has a short lifetime (Yuan et al., 2021). The typical requirement of OBC including its power density and efficiency for each stages are highlighted in Yuan et al. (2021). The bidirectional and unidirectional charger are further classified as single stage and two-stage charger. The universal on board two-stage charger including a front-end AC–DC converter and back-end DC–DC converter is shown in Fig. 1. To filter out high-frequency noise, the output EMI filter is supplied to an AC–DC converter which has the facility of power factor correction. To maintain the ripple magnitude in the output of the AC–DC converter within the specified limit, a dc-link capacitor of a suitable value is connected across the output of the AC–DC converter. The output of the DC-link capacitor is supplied to the isolated DC–DC converter which is used to charge the battery of the EV. charges the EV battery. The outputs of the front-end AC–DC converter and back-end DC–DC converter are regulated with the help of the controller. While isolated DC–DC converter provides galvanic isolation. Galvanic isolation is often imposed between the high voltage side of the battery pack and the grid-side dc link for safety purposes. However, the vehicle's chassis and low-voltage side should be galvanically isolated from the high voltage battery.

Depending upon the output power delivered by two-stage EV chargers, these are categorized as Level-1, level-2 and level-3 chargers. Level-1 and level-2 chargers are on-board chargers while level-3 is off-board charger (Yuan et al., 2021; Williamson et al., 2015; Yuan et al., 2021). A detailed review of on-board charges is discussed in Yuan et al. (2021) along with the configurations, industry standards and commercial list of bidirectional chargers. The issues associated with EV battery, chargers and traction motor drives are discussed in Williamson et al. (2015). The review on bidirectional converters based on configurations with required industry standards is discussed in Yuan et al. (2021).

The off-board chargers have the significant benefit of being less limited by size and weight while having the quickest charging time as compared to level-1, level-2 on-board chargers. Level −1 on-board chargers are used in applications like home, office parking while level-2 on-board chargers are used in public or private outlets. Level −3 off-board chargers are preferred for commercial buildings (Khaligh and D'Antonio, 2019; Mohammed and Jung, 2021). Table 2 gives details of various charging levels of on-board and off-board chargers and the corresponding capacity of the EV with which these EVs can be charged. The EV charger classification and the type of plug required for each level is discussed

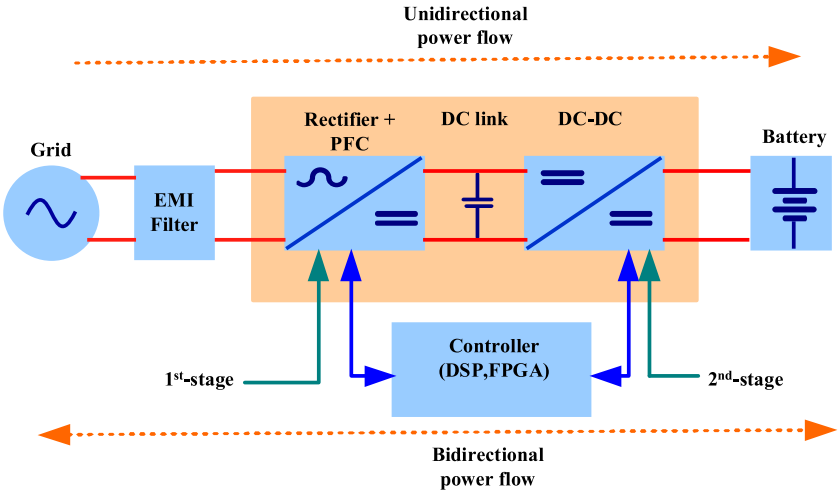

Fig. 1. General block diagram of charger.

Table 1
Charger classification.

Category of classification	Types
Topology	1. Dedicated 2. Integrated
Mounting	1. On-Board 2. Off-Board
Connection type	1. Inductive 2. Conductive
Electrical connection	1. AC 2. DC
Direction of power flow	1. Unidirectional 2. Bidirectional

in Khaligh and D'Antonio (2019). A detailed classification of wired and wireless charging methods are discussed in Mohammed and Jung (2021).

Some of the EV models available in the market with their rated battery capacities are also included in Table 2. Citroen vehicle (2016) has a battery capacity of 16 kWh that can be charged using power level-1. The battery capacities of Hyundai IONIQ (2016) and Ford Focus (2017) are 30.5 kWh and 33.5 kWh, respectively and can be charged using level-2. The Level-3 is used for fast charging of BMWi3 (2018) and Citroen C4 (2021) with respective battery capacities of 42.3 kWh and 50 kWh (Yilmaz and Krein, 2013; Pod-Point, 2021).

The objective of the EV charger is to ensure fast charging of the battery fulfilling requirements of simple design, galvanic isolation, low weight, small size and cost effectiveness. However, the design of EV chargers suffers from key challenges like low efficiency, nonavailability of isolation, high cost and low power density. By increasing the switching frequency of the converter, the values of passive elements can be reduced. However, increment in switching frequency leads to increment in switching losses during turn-on and turn-off switching devices. A further issue with such a system is the reverse recovery losses and noise caused by the output rectifiers' high di/dt and dv/dt ratios. To overcome these limitations, resonant circuits and soft switching techniques are widely used.

Electric vehicles are facing several technical challenges in their full adaptation, e.g., high charging time, range anxiety, high losses and poor efficiency of available EV chargers. Resonant converters recently gained popularity owing to their capabilities to address these EV charger's challenges. Resonant converters can help achieve fast charging, and decreased losses by offering zero voltage and current switching, leading to minimizing range anxiety. Furthermore, resonant converters also provide galvanic isolation, soft switching and high-power density; key requirements in an EV charger. In addition, resonant converters can also help to achieve V2G, and V2H mode of operations of EV chargers due to their capability of allowing the bidirectional flow of power. Various types of EV chargers that employ resonant converters are discussed in Bai et al. (2020), Kwon and Choi (2017), Lee et al. (2017), Xuan et al. (2021) and Pandey and Singh (2019). The series resonant converter (SRC) based charger is discussed in Bai et al. (2020). This topology is the bidirectional type and provides galvanic isolation, soft-switching, and high-power density. However, the control strategy used for Vehicle-to-Grid (V2G) operation which is required for the exchange of active (Bai et al., 2020). In Kwon and Choi (2017) a half-bridge SRC that operates in Grid-to-Vehicle (G2V), V2G, and Vehicle-to-Home (V2H) modes of operation is discussed. In addition, the control schemes are also highlighted. A PWM-RC series resonant converter for V2G mode (Lee et al., 2017). An LLC and CLLC converter is also used in EVs as discussed in Xuan et al. (2021) and Pandey and Singh (2019).

Due to the advantages mentioned above, resonant converters are considered as an integral part of an EV charging station.

However, the increased penetration of EVs may cause fluctuation of load, and the scheduling of the charging of electric vehicles in charging stations may become difficult. A bi-level optimum dispatching model is discussed in Li et al. (2021a) for the charging station to overcome this issue. The integrated demand response program is used which is designed to maintain a balance between energy supply and demand while keeping user satisfaction within an expected range.

Modulation techniques used for resonant converters are classified as Pulse width modulation (PWM) and Frequency modulation (FM) techniques. However, frequency-modulated resonant converters provide several advantages over traditional pulse width modulated converters, including (a) lower switching losses and high efficiency. (b) ability to work at a higher switching frequency, which helps in reduction of the size of magnetic components and thus enhances power density, and (c) zero-voltage switching ability, that could resolve the issues of electromagnetic interference.

The continuous growth is being observed in the area of EVs which necessitates the requirement of DC–DC converters having a wide range of dc output voltage (Musavi et al., 2013a; Fang et al., 2015; Beiranvand et al., 2011; Wu et al., 2016; Wang and Li, 2018; Xue et al., 2021). The use of LLC converter for battery application is discussed in Musavi et al. (2013a) and the procedure for the

Table 2
Details of Charger.

Level types	Voltage	Current	Output power level	Vehicle capacity
Level-1 (on-board)	120 V_{ac}	12 A	1.4 kW	16–50 kWh
1-phase	230 V_{ac}	20 A	1.9 kW	1. Citroen C-zero (2016) Battery capacity- 16 kWh
Level-2 (on-board)	240 V_{ac}	17 A	4 kW	3–50 kWh
1-phase				1. Hyundai IONIQ (2016)
3-phase	400 V_{ac}	32 kW	8 kW	Battery capacity- 30.5 kWh 2. Ford Focus Electric (2017) Battery capacity- 33.5 kWh

optimal design of LLC converter is discussed in Fang et al. (2015) and Beiranvand et al. (2011). A modification in rectifier circuit of LLC (Wu et al., 2016) or by changing modulation scheme like PWM, phase-shifted for LLC converter is suggested for wide-output voltage applications in Wang and Li (2018) and Xue et al. (2021). A novel parallel-loaded resonant converter is suggested in Kim et al. (2018) which is mainly used for wide-output-voltage applications.

The voltage gain of a frequency modulated LLC based resonant converter should be high over the wide range of the switching frequency, f_s. The resonant converter loses its ZVS capability if switching frequency, f_s is less than the resonant frequency, f_r. However, if the value of f_r is greater than f_r, the voltage regulation of resonant converter becomes poor due to the impact of junction capacitance, (C_j) of secondary-side rectifying diodes. The efficiency of LLC based resonant converter decreases rapidly with an increase in the difference between f_s and f_r (Kim et al., 2018). Furthermore, the size of magnetic components is constrained by the lower bound on f_s. From the above discussion, it is observed that the design of LLC based resonant converter suffers from various challenges. To overcome above-mentioned limitations, various techniques are discussed in the literature which is based on the following four methods:

1. By adjusting parameters of the tank circuit.
2. By reconfigurable circuits such as full-bridge, half-bridge, voltage doubler, voltage quadruple etc. on the secondary side of isolation transfer.
3. By using reconfigurable circuits such as full-bridge, half-bridge etc. on the primary side of isolation transfer.
4. By modifying the control and modulation strategies

By using a modified tank circuit in resonant converters (Beiranvand et al., 2011; Wu et al., 2016) or the output rectifier (Wang and Li, 2018; Xue et al., 2021), high efficiency can be achieved over a wide range of output voltages. Reconfigurable resonant converter based topologies of DC–DC converters are suggested in Shen et al. (2019), Li et al. (2020a) and Shang and Wang (2018), which ensure a wide range of output voltages. In Shen et al. (2019) a reconfiguration in the series converter is proposed. A two-interleaved LLC converter on the secondary side with PWM scheme. The efficiency of the converter is 97.31% (Li et al., 2020a). A voltage quadrupler rectifier in LLC converter is suggested (Shang and Wang, 2018). In Metwly et al. (2020), various topologies of integrated on-board chargers used for EV applications are discussed. The control techniques used for the charging EVs, technical challenges and types of different converters used in integrated chargers are also highlighted. The current status and future trends of bidirectional on-board chargers are discussed in Wang et al. (2019). Moreover, various configurations of on-board chargers like two-stage and single-stage are also discussed in detail. In Wang and Khaligh (2013), different resonant converter topologies like series, parallel, series–parallel, LCC and LLC based half-bridge topologies that are capable to charge a Li-ion battery having a power rating of 3.2 kW and voltage 360 V used in plug-in-EV (PEV) are compared. The two-element resonant converter topology used for wireless power transfer (WPT) for EVs is discussed in Mude and Aditya (2019). However, the classification of resonant converter used in EV charger application are not discussed (Severns, 1992).

This paper deals with a state-of-art literature survey of resonant converters used in EV charging applications. The advantages and limitations offered by these converter typologies, their efficiencies and the number of passive elements required in a given resonant converter topology used in unidirectional and bidirectional chargers are clearly highlighted. In addition, design steps required for optimizing the size of magnetic components are discussed. Various industry standards like IEC, ISO, IEEE used in EV charging as per the type of connectors used in EVs are listed. The main contributions of the paper are listed below:-

1. A detailed classification of resonant converters used in EV chargers is included.
2. A comparison table of unidirectional (1 kW, 1.5 kW, 3.3 kW) and bidirectional (3.5 kW, 6.6 kW) chargers based on efficiency, number of resonant elements, resonant frequency and battery voltage is also included. This table can be used as a guideline to design the first stage and second stage of EV charger of a given power rating and direction of power flow (unidirectional and bidirectional power flow mentioned in the literature). Moreover, the contribution and limitations of various converter topologies used first and the second stage are included. The dominant area of future research is also identified.
3. It highlights various modulations schemes, control schemes for LLC and CLLC converters. Moreover, the control schemes required for the exchange of active power (P) and reactive power (Q) in the V2G mode of operation are included.
4. The list of commercial companies which provide EV charging facilities at various places like homes, commercial buildings, highway corridors etc. is also included in this paper.

2. Resonant converter classification

The schematic of resonant power converters (RPCs) including six stages is shown in Fig. 2. The first stage is the input source which can be a voltage or a current source. The second stage is a bridge inverter which can be a half-bridge or full-bridge inverter. The output of the second stage is supplied to the Nth order resonant tank circuit formed by inductors and capacitors. Here, N (Where $N = 0,1,2, \cdots, N$) indicates the total number of inductors and capacitors connected in the resonant tank circuit. The next stage is the transformer which is used to isolate one stage from another stage. In addition it, this can be also be used for the step-up and step-down operation of system voltage. The output of the isolation stage is supplied to the bridge rectifier stage which can be a full-bridge or half-bridge rectifier. The output of the bridge rectifier stage is supplied to the filter stage that includes either a low pass filter or a high pass filter. The output of the filter stage is used to charge the battery connected in EV (Tan and Ruan, 2016).

The soft switching based DC–DC converters. They are further categorized as resonant power converters (RPC)s, zero transition converters (ZTC), qausi-resonant and multi-resonant converter (QRC & MRCs) shown in Fig. 3. The RPCs are classified

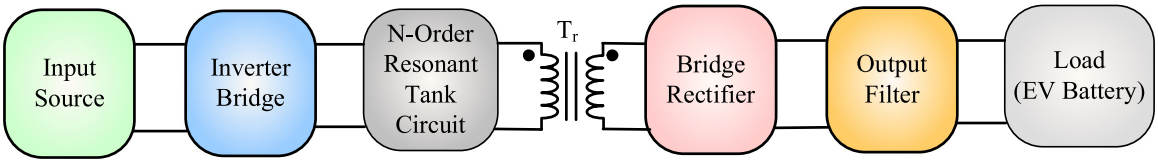

Fig. 2. The structure of resonant power converter.

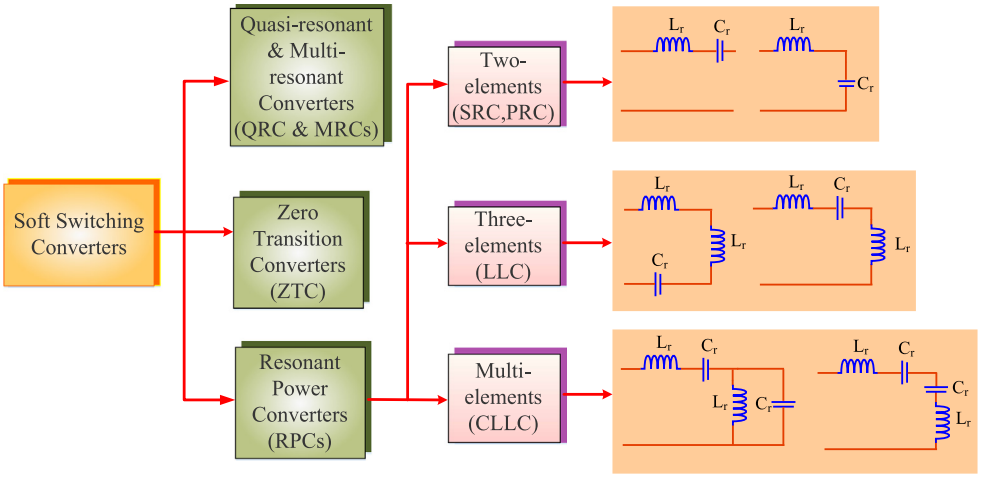

Fig. 3. Classification of soft switching converter.

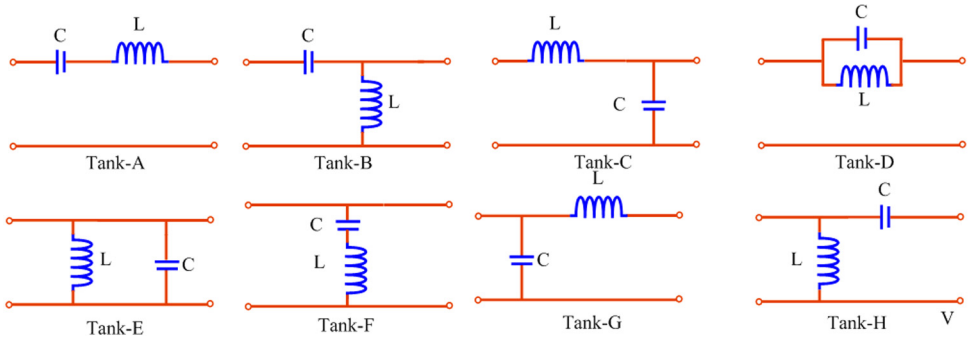

Fig. 4. Two-element eight combination.

as two-element (second-order), three-element (third-order) and multi-element (higher order) types of RPCs as shown in Fig. 2. Two-element RPC is a second order resonant tank circuit which includes single inductor and single capacitor. Depending upon the connection of either voltage or current source at the input port, there are eight possible configurations of two-element RPCs as shown in Fig. 4. The configurations shown in Fig. 4 tank A, tank B, tank C and tank D are used for voltage source resonant converters, while the configurations shown in Fig. 4 tank E, tank F, tank G and tank H are used for current source resonant converters (Tan and Ruan, 2016; Huang et al., 2011). The tank circuit of voltage source configurations shown in Fig. 4 tank A behaves like a band pass filter. Therefore, it is called series resonant converter (SRC) or series resonant frequency (SRF). The configurations shown in tank B and tank C are called parallel resonant converters (PRC) or parallel resonant frequency (PRF) they behaves like high pass filter and low pass filter. The configuration shown in Fig. 4 tank d behaves like a notch filter and is called Notch Resonant Frequency (NRF) converter.

The SRC suffers from the limitation that a wide range of frequency variation is required to regulate output voltage. At no load or light load condition, the regulation of output voltage becomes difficult. The PRC has low efficiency and high circulating energy at light load condition. In addition, for high voltage and contactless energy transfer applications, the SRC and PRC cannot utilize parasitic components like magnetizing inductor in isolation transformer (Mude and Aditya, 2019; Tan and Ruan, 2016). To overcome this limitation, a three-element or higher order resonant tank circuit based resonant converters are used as suggested in literature. The three-element resonant tank circuits are derived by adding the third element to two-element resonant tank circuits. It combines the advantages of both SRC and PRC. The three element based resonant converter can be further classified on the basis of resonant tank circuit including two inductors and one capacitor (LLC) and two capacitor and one inductors (CCL). Based on LLC and CCL resonant tank circuits, there are thirty six possible configurations of three element resonant converters. However, only twenty six out of these thirty six configurations of resonant converters are able to resonate shown in Fig. 5.

The following criteria is used to form a resonant converter based on three element resonant tank circuit (Tan and Ruan, 2016):

1. When the input of the resonant tank circuit is an open circuit on replacing inductors by an open circuit and capacitors as a short circuit. This give rise to the development

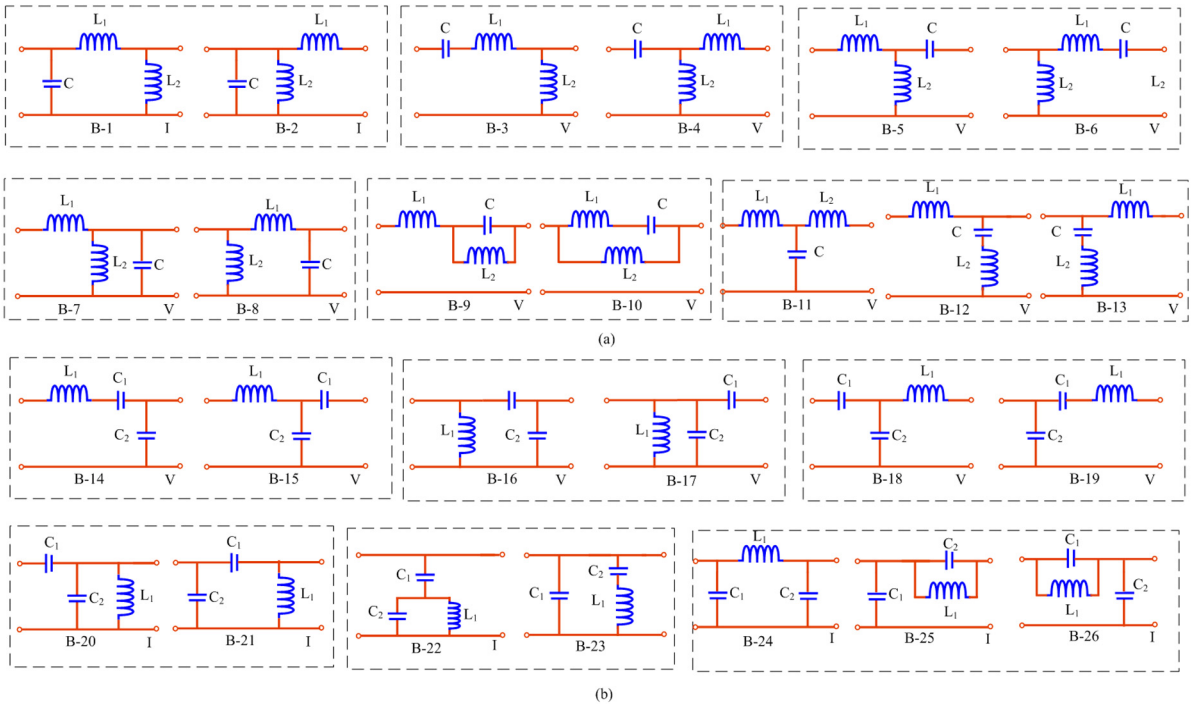

Fig. 5. Three-element twenty-six combination (a) Two-inductors and one capacitor tank circuit (b) Two-capacitors and one inductors tank circuit. (In the lower right corner, the resonant tank that is suited for input voltage source and input current source is designated by *V* and *I*, accordingly.

of a resonant converter based configuration with voltage source used as input.

2. When the input of the resonant tank circuit is a short circuit by replacing inductors to be open circuits and capacitors as a short circuit. That develops a resonant converter with input as the current source.
3. If the input of resonant tank circuit is directly connected to the output, this converter cannot be used as a resonant converters.
4. If the input is voltage source the input impedance of resonant tank circuit should be infinity at high frequency to limit the high-frequency input current of the resonant tank circuit. At high frequency, it will approximate a sinusoidal wave.
5. When the input source is a current source, the input impedance should be zero at high frequency to restrict high-frequency components of input voltage of resonant tank circuit. At high frequency, it will approximate a sinusoidal wave.

The most commonly used configuration of resonant converter based on LLC resonant tank circuits including voltage and current sources are shown Fig. 5a. Similarly, the configuration of resonant converter based on CCL resonant tank circuits including voltage and current sources are shown Fig. 5b.

The three-element (third-order) based resonant converters have more advantages like it can operate in zero-voltage-switching (ZVS) region for large load variation, lower stress on the diodes than two-element. However, switching and conduction loss increases when the input voltage is high in a three-element resonant converter. Resonant converters including tank circuits with four, five or more reactive elements are included in the category of multi-element (higher-order) resonant converters. With a four-element resonant tank, the circuit lead to 182 topologies. Class-1, 2 has 42 topologies and class-3, has 98 topologies (Batarseh, 1994). The four-element resonant tank is further grouped into three classes they are as follows:

1. Three capacitors and one inductor (Class-1)
2. Three inductors and one capacitor (Class-2)
3. Three capacitors and one inductor (Class-3).

The generalized configurations of resonant tank circuits with four-element are shown in Fig. 6. The various variants of four-element tank circuits are discussed in Salem and Yahya (2019) and Outeiro et al. (2016). The relative advantage and disadvantages of resonant converters based on two-element, three-element and multi-element tank circuits are discussed in Table 3.

2.1. Series resonant converter

The schematic of the series resonant converter (SRC) is as shown in Fig. 7a. The SRC includes a half-bridge inverter, two-element resonant network, isolation transformer and rectifier. The half-bridge inverter consists of two switches including its body diode and parasitic capacitors. The resonant tank circuit contains resonant inductor, L_r and capacitor, C_r. The reactive elements, L_r and C_r are placed in series with the transformer winding and hence called as a series resonant converter. The resonant tank circuit and the load connected at the output of the rectifier are in series. Here, the tank circuit and load act as voltage divider. The impedance of the resonant tank can be changed by adjusting the frequency of the driving voltage, V. The input voltage is divided between the load and impedance of the resonant tank. The SRC acts as a voltage divider circuit. Therefore, the DC gain of SRC is always less than unity. The value of the impedance of the tank circuit at the resonant frequency is small. Therefore, the value of the output voltage of the resonant converter is equal to its input voltage. Hence, the value of gain of SRC is maximum at the resonant frequency (Yang, 2003; Steigerwald, 1988). The SRC converter includes a capacitor on the primary side of the transformer that will block the block dc component of primary current (Steigerwald, 1988). Therefore, a low selectivity is observed in voltage gain characteristics of SRC at no-load conditions. For this condition, the voltage gain curve appears to be a horizontal line. Therefore, SRC cannot operate at no-load condition is one of the limitations of the SRC converter.

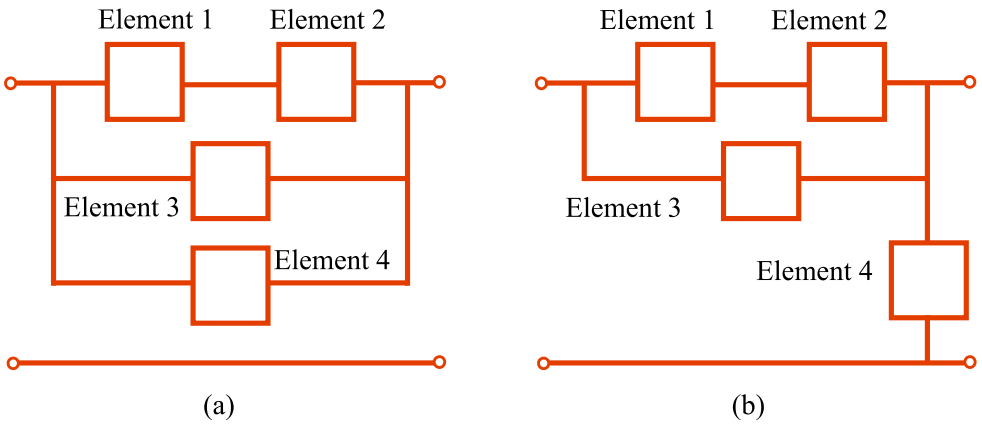

Fig. 6. Four-element (multi-element) generalized tank circuit.

Table 3
Advantages and disadvantage of two-element, three-element and multi-element (Salem and Yahya, 2019; Outeiro et al., 2016).

	Two-element		Three-element	Multi-element
	SRC	PRC	LLC	CLLC
Advantage	It is distinguished by its simplicity, inherent blocking by a capacitor of the isolation transformer and the ability to integrate the HF transformer's leakage inductance in the RTN.	Simple, no-load regulation ability, low output ripple current.	No-load regulation. With a relatively small switching frequency variation, the output voltage can be controlled from zero to maximum under any load condition. Low circulating current, switching losses	Low switching losses
Disadvantage	Light load regulation, high circulating energy, and turn off current at high input voltage are the main issues.	The lack of inherent blocking by capacitor of the isolation transformer and the rise in current because of the rise in input voltage are the two primary drawbacks. The main issues are excessive circulating energy and current turnoff.	At frequencies near to f_{rs}, the LLC topology cannot run effectively with an open circuit, and at frequencies close to f_{rp}, it cannot run effectively with a short circuit.	As the number of reactive elements increases configuration becomes complex for analysis, increases cost and size

The other limitation is that the output filter should be able to handle high ripple current. Therefore, SRC is not suitable for low-voltage high current applications.

2.2. Parallel-resonant-converter

The schematic of the parallel resonant converter is shown in Fig. 7b. In PRC, either one of the reactive components or both are connected parallel to the load. This configuration is called a parallel resonant converter (Yang, 2003; Steigerwald, 1988). The primary side of the transformer contains a capacitor and an inductor is used on the secondary side to match the impedance. The limitation of the SRC converter is resolved by using PRC that in the no-load condition it is able to regulate the output voltage. It suffers from the limitation that the magnitude of circulating current increases with an increase in input voltage. The magnitude of circulating current is high as compared to SRC.

2.3. Series–parallel resonant converter

The schematic of the series–parallel resonant converter is shown in Fig. 8. It includes three reactive elements. The resonant tank of SPRC is a hybrid formed by the combination of SRC and PRC. An output filter inductor is added to the secondary side, similar to the PRC, to match the impedance (Yang, 2003). This arrangement eliminates the drawbacks of SRC and PRC like no-load regulation and flow of circulating current. This can be achieved by proper design and selection of resonant components. This series–parallel resonant converter can regulate the output voltage in no-load condition only if the value of C_p is not too small. If the value of C_p is too small, it will behave like an SRC (Steigerwald, 1988).

2.4. LLC converter

Advantages of the series and parallel resonant converters are combined in the LLC resonant converter. The additional benefits of the resonant converters (especially LLC type) imparted to EVs are elaborated in Fig. 9. The LLC resonant converter helps to achieve the zero-voltage switching (ZVS) turn-on and zero-current switching (ZCS) turn-off operation. In addition, the higher power density is achieved by operating at a higher frequency which will reduce the size of the transformer. Moreover, the transformer also provides galvanic isolation. The resonant converter generates a wide-output range of voltages. By varying the switching frequency there is a change in the impedance of the resonant components which will result in a change in the gain of the converter. The voltage and current waveforms of the diode rectifier do not contain any spikes. Hence it has low EMI and harmonic pollution.

Fig. 10 shows the schematic of the half-bridge LLC converter. It is divided into five parts which are a half-bridge inverter, the resonant tank, transformer with turns ratio of n:1 and the center-tapped rectifier circuit, output capacitor. The load to the

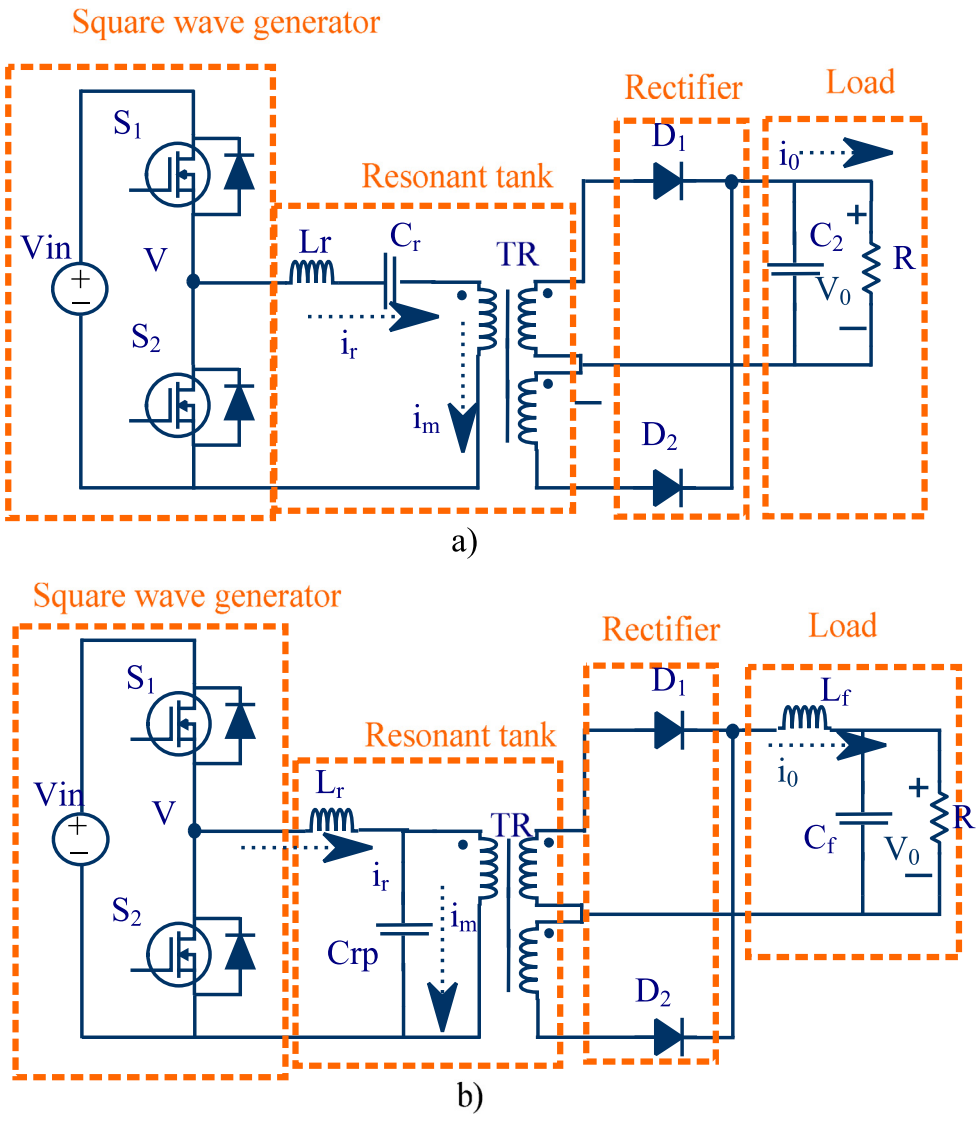

Fig. 7. (a) Half-bridge series-resonant converter (b) Half-bridge parallel-resonant converter.

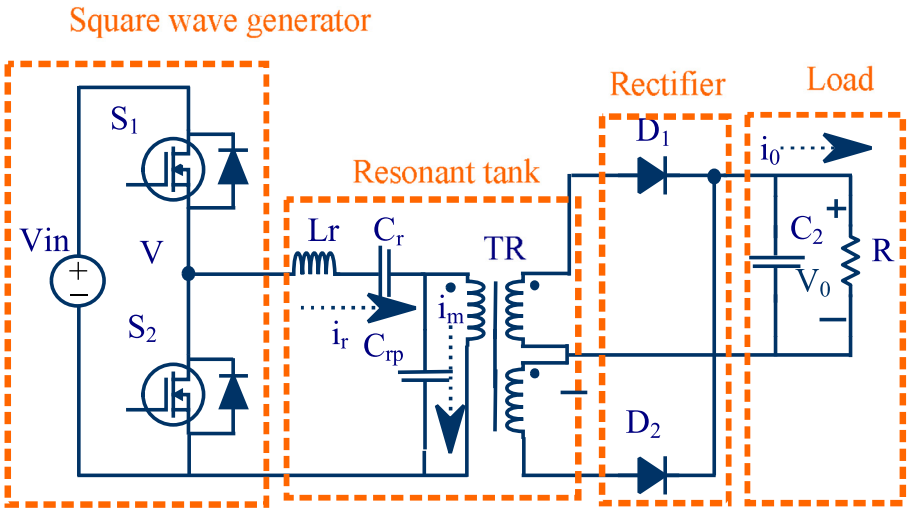

Fig. 8. Half-bridge series–parallel converter.

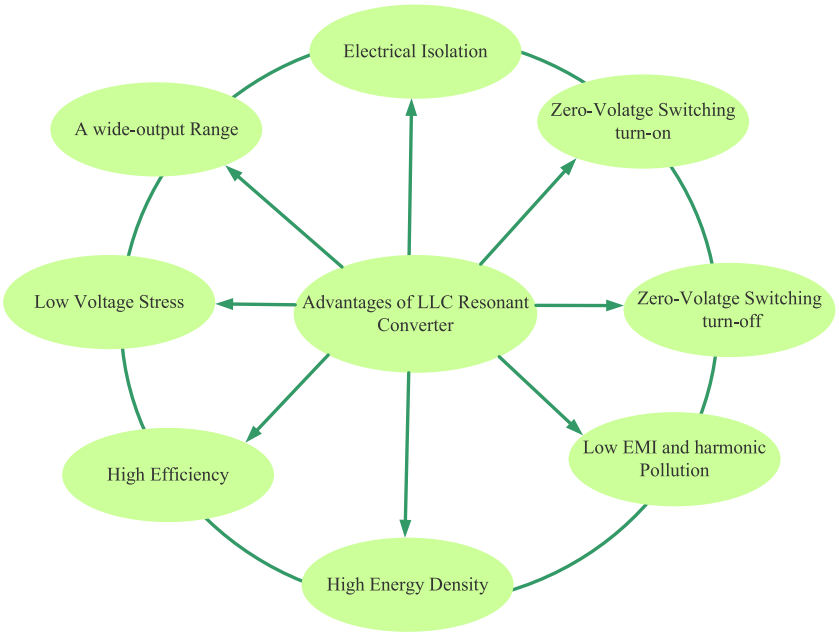

Fig. 9. Benefits of LLC converter.

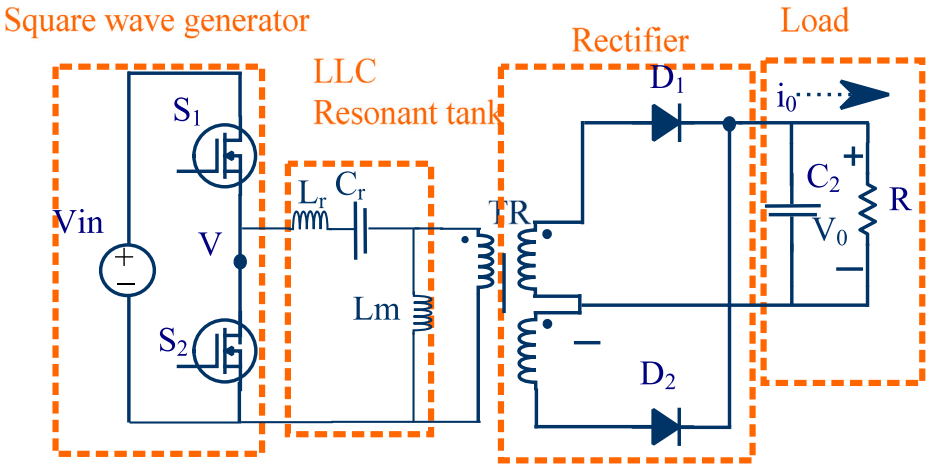

Fig. 10. Half-Bridge LLC converter.

LLC converter is the battery represented as a resistive load. The difference between series based resonant converter and LLC resonant converter is the presence of magnetizing inductance L_m. The LLC converter has three resonant component, L_r, C_r and L_m. Here, L_r, C_r are the resonant inductor and capacitor and L_m is the magnetizing inductance. Input to this tank circuit is a half-bridge inverter configuration. Automatic flux balancing is possible due to the presence of a capacitor in series with the power path. This LLC resonant converter operates in variable frequency mode. It has two resonant frequencies. The first resonant frequency of the LLC converter corresponds to the inductor, L_r and the resonant capacitor, C_r and the resonant frequency of LLC converter correspond to L_m plus L_r and C_r. The two frequencies are defined as given below:-

$$f_1 = \frac{1}{2\pi\sqrt{L_r C_r}} \tag{1}$$

$$f_2 = \frac{1}{2\pi\sqrt{(L_r + L_m)C_r}} \tag{2}$$

$$Q = \frac{\sqrt{(L_r/C_r)}}{R} \tag{3}$$

The LLC resonant converter with DC-characteristics is discussed (Zeng et al., 2020). It is observed that the peak of the gain varies as the load changes. For light load condition, the peak approaches near to the resonant frequency, f_2, while for heavy load condition, the peak of the gain approaches to the resonant frequency, f_1. In addition, the gain is always unity at the resonant frequency, f_1 regardless of the change in load. The characteristic waveform during light load conditions resembles PRC. On the other hand, during heavy load conditions, it resembles SRC. The important feature of this converter is that the dc-gain can be more than or lower than unity.

2.4.1. Working of LLC

For the operating region lying between frequencies, f_1 and f_2, the load condition will determine whether the converter is working in ZVS or ZCS condition. The working of the LLC resonant converter is shown in Figs. 11 and 12. The inductor currents are I_r and I_m, which are flowing through the reactive elements, L_r

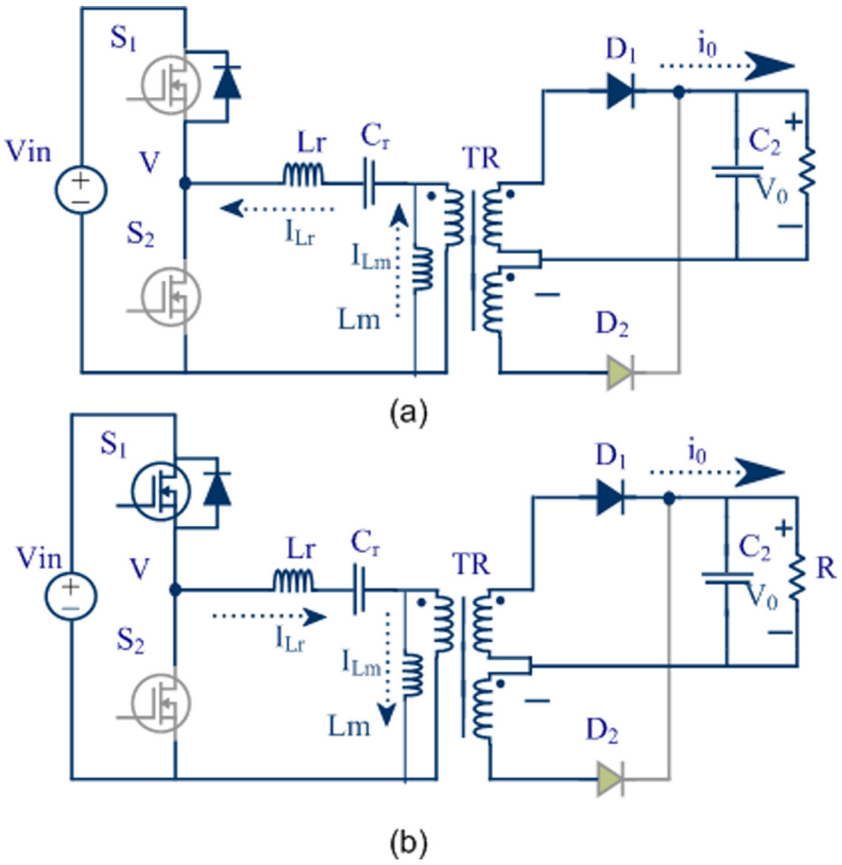

Fig. 11. Working of Half-Bridge LLC converter (a) Mode 1 (b) Mode 2.

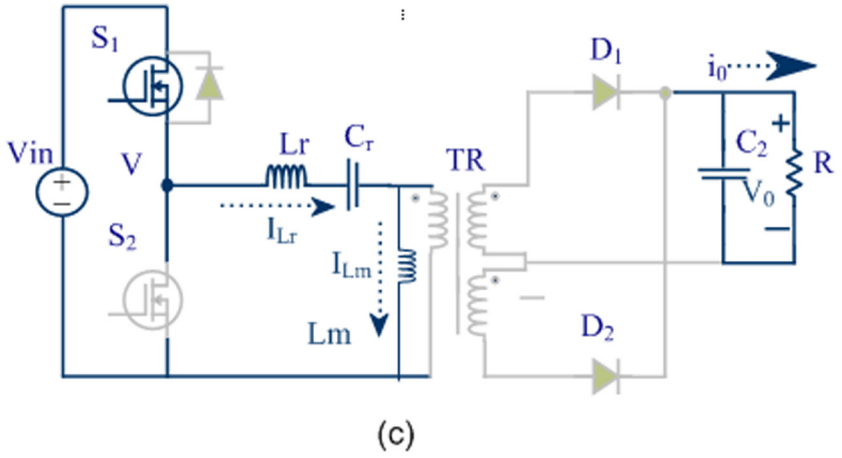

Fig. 12. Working of Half-Bridge LLC converter (c) Mode 3.

and L_m, respectively. It operates in three modes. Mode 1 starts when switch S_2 is in off-state. At that time, the inductor current I_r, which is flowing through the reactive element, L_r is negative. In mode II, the inductor current, I_r is positive and S_1 is in on-state, while the mode III starts when both the inductor current, I_r and I_m are same (Yang et al., 2002).

The analysis of the resonant converter including a resonant tank circuit with three reactive elements is quite challenging. The study of LLC resonant converters (Lazar and Martinelli, 2001) ensures correctness. However, due to the complexity of the system, it cannot be easily exploited to provide a useful design approach. For operating conditions at and above the resonance frequency of resonant tank circuit, the fundamental harmonic approximation (FHA) technique produces satisfactory results (Duerbaum, 1998). For a wide-output range, the LLC converter with FHA is discussed in Lazar and Martinelli (2001). Here, the range is expanded for frequency above the resonant frequency. However, the ZCS for rectifier diodes is missing when compared to the zone below resonance, there are more diode reverse recovery losses (Fang et al., 2012). In the zone below resonance, the FHA is still valid. However, the results produced by FHA are less accurate. As a result, it is suitable for qualitative analysis but not for optimal design procedures. The operating mode analysis in Fang et al. (2011a) and Fang et al. (2011b) is used to build optimal design approaches. These methods can produce excellent design

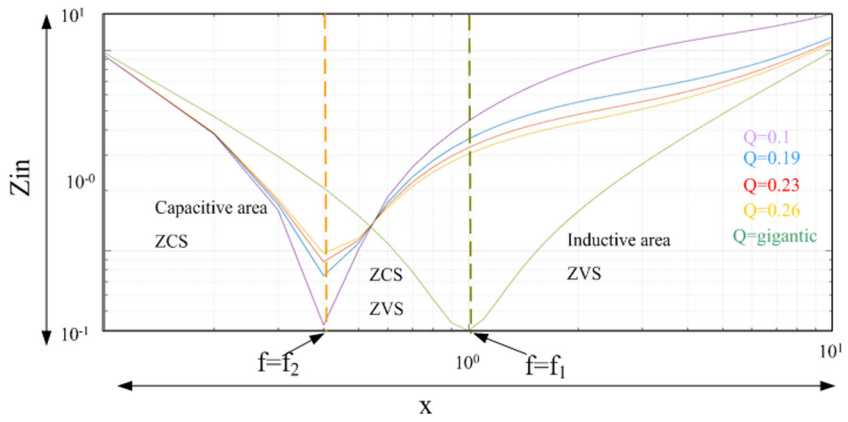

Fig. 13. Impedance and frequency plot for Half-bridge LLC converter.

Table 4
Comparison between region-1, 2 and 3.

	Region-1 ($f_s < f_r$)	Region-2 ($f_s > f_r$)	Resonant region ($f_s = f_r$)
Turn-off loss (primary switches)	⋆	⋆ ⋆ ⋆	⋆
di/*dt* of diodes turn-off	⋆	⋆ ⋆ ⋆	⋆
Circulating energy	⋆ ⋆ ⋆	⋆ ⋆	⋆
Conduction loss	⋆ ⋆ ⋆	⋆ ⋆	⋆
Switching loss	⋆	⋆ ⋆ ⋆	⋆
Harmonics	⋆	⋆ ⋆ ⋆	⋆
Complete performance	Moderate	Moderate	Good

⋆ -Low; ⋆ ⋆ -Medium; ⋆ ⋆ ⋆ -High.

outcomes. However, these techniques necessitate the use of complex math tools. In Adragna et al. (2008), a simple and accurate design-oriented model is suggested and a step-by-step design technique that ensures the majority of the benefits of an LLC converter throughout the wide output voltage range is not discussed. Comparison between region 1, 2 and 3 are discussed in Table 4.

The operating frequency of the resonant converter affects the input impedance. The expression for input impedance is given by,

$$Z_{in}(x,k,Q) = Z_R\left(\frac{Q*x^2*k^2}{1+x^2*k^2} + j\left(x - \frac{1}{x} + \frac{x*k}{Q*x^2*k^2}\right)\right) \quad (4)$$

where, f_1 is the frequency of the converter. x is defined as the ratio of switching frequency f_s and f_1, while k is the ratio of magnetic inductance and leakage inductance of the transformer. The characteristic impedance of the resonant circuit is given by (4). The input impedance can be inductive or capacitive as shown in Fig. 13. L_r and C_r the resonant inductor and capacitor while is the L_m magnetizing inductance.

$$x = f_s/f_1 \quad (5)$$

$$k = L_m/L_r \quad (6)$$

$$Z_R = \sqrt{(L_r)/(C_r)} \quad (7)$$

The equivalent circuit of LLC converter is shown in Fig. 14 and first harmonic approximation circuit is shown in Fig. 15. Here, $V_1(t)$, $i_{p1}(t)$, $v_{p1}(t)$, $i_{p2}(t)$ represent FHA components of supply voltage $V_1(t)$. The LLC converter is modeled as follows using the first harmonic approximation (FHA) to simplify the analysis as shown in Fig. 15

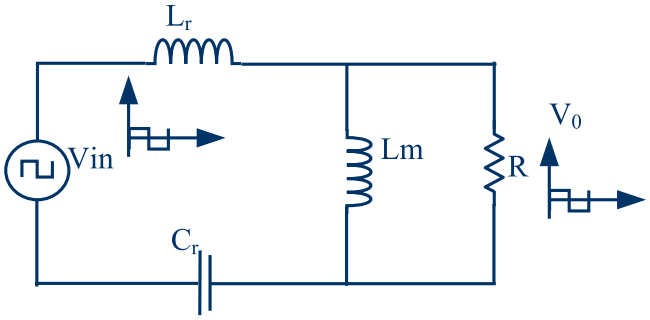

Fig. 14. Equivalent structure of LLC.

2.5. CLLC converter

The LLC converter has an unsymmetrical resonant tank circuit. However, this issue is resolved by using a CLLC converter. The full-bridge CLLC converter is shown in Fig. 16. It has four resonant components, C_{pr} L_{pr} L_{rs} C_{rs}. It is controlled by a variable frequency that covers a wide area of soft switching region during light load conditions. It offers higher efficiency. However, its design and control is complex. A 6.6 kW CLLC resonant converter with an efficiency of 97.85% is suggested in Zhang et al. (2020). A comparative study between half-bridge and full-bridge CLLC converter is carried out in He and Khaligh (2016). The half-bridge has high current stress and power density is also high and low cost as compared to the full-bridge. A comparative analysis shows that the ZVS region is reduced because of the parasitic capacitance of switches (Siebke et al., 2019; Zou et al., 2017a).

3. Modulation control schemes

Modulation Control Schemes The efficiency of resonant converters is decided by the power semiconductor switches and passive components. However, the modulation schemes adopted for resonant converters have a significant impact on the efficiency of these converters. The modulation schemes which are mainly used for resonant converters are variable frequency (VF), fixed frequency, and optimal trajectory control schemes (Youssef and Jain, 2004).

3.1. The variable frequency control scheme

This scheme is used to control the output voltage of the resonant converter. In this scheme, voltage control is achieved by varying the switching frequency fs above the resonant frequency fr. The switches in one leg of the full-bridge resonant converter

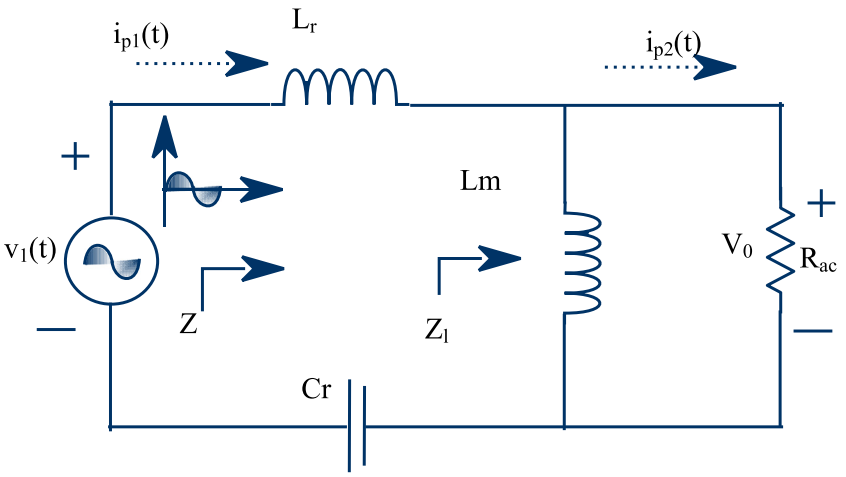

Fig. 15. Equivalent structure of based on FHA.

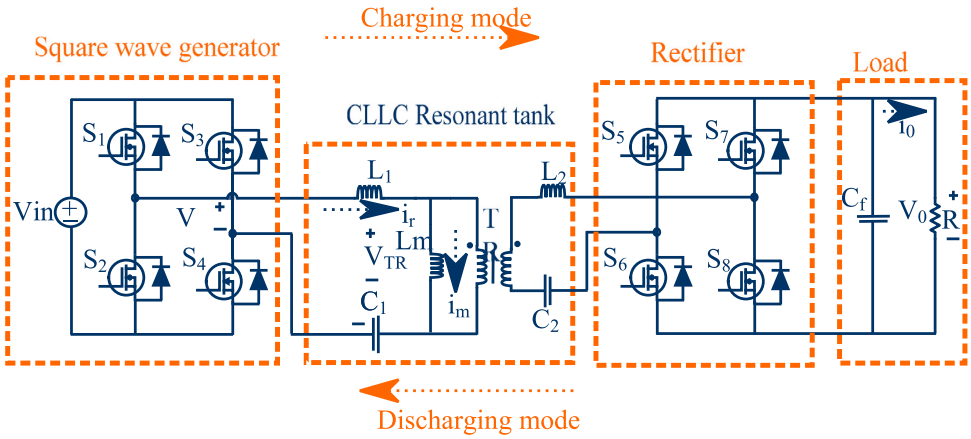

Fig. 16. Bidirectional full-bridge CLLC converter configuration.

are operated at 50% duty cycle and a phase shift of 180 degrees is maintained among the control signals of the other leg of the bridge. In this scheme, the on-time of the switch is maintained at a constant value while the off-time is variable in nature. Consequently, this scheme leads to a poor transient response of the converter. The variable-frequency scheme is further classified as self-sustained oscillation controller (SSOC) and self-sustained phase shift modulation (SSPSM).

3.2. Fixed frequency scheme

In a fixed frequency control scheme, the resonant converter is operated in fixed frequency with an objective to ensure the ZVS operation of the resonant converter. However, the resonant converters loss their ZVS capability under light load conditions and wide range of variations in input voltage under this control scheme. This scheme is further classified into three categories which are (a) schemes including phase-shift modulation (PSM), (b) asymmetrical pulse width modulation (APWM) and (c) asymmetrical clamped mode (ACM). The PSM control scheme is applicable to only full-bridge converters. The phase angle, Θ between the control signals applied to two switches in a leg is (180-Θ) degree and the duty ratio for both switches is fixed at a value of 50%. The operation of resonant converters is ensured for variable the duty cycle (d) and the switching frequency f_s is selected above the resonant frequency f_r. As a result, one inverter leg will undergo zero current switching (ZCS) and the other will undergo (ZVS) zero voltage switching.

3.3. Self-sustained oscillation modulation (SSOC)

The main aim of this scheme is to control switching frequency so that it simultaneously ensures both voltage regulation and ZVS of the resonant converter. It consists of two control loops which are termed as inner loop and outer loop. The function of the inner loop is to adjust the phase shift between the resonant current (i_s) and inverter output voltage (V_{ab}) to ensure that is lags (V_{ab}) while the outer loop regulates the output voltage as per the reference value.

3.4. Self-sustained phase shift modulation (SSPSM)

This scheme is formed by the combination of SSOC and PSM so as to improve the performance of the variable frequency control scheme. The objective of this scheme is to control the switching frequency and width of PWM pulses simultaneously which ensures that output voltage is regulated and the ZVS operation of the converter is maintained. This is achieved with the help of the inner loop and outer loop. The functionality of these loops is the same as that of loops mentioned in SSOC.

3.5. Optimal trajectory control

It is also known as linear quadratic regulator (LQR). This scheme is a special case of state-plane trajectory in which the controller follows a certain path that holds resonant tank energy within fixed bounds. The first step is to derive a state–space model of the circuit at one operating point. The second step is

to calculate the LQR for that operating point. This control scheme has a fast transient response subsequently followed by the SSPSM, SSOC, then by PSM and in last by VF controller.

If the switching frequency of the resonant converter is selected above the resonant frequency, it generates high switching losses. The increased switching losses leads to an increment in the temperature of the device which in turn increases conduction losses. In a similar fashion, the circulating current flowing among the converters further increases the conduction losses. The control strategies for resonant converters should be selected in such a way that improves the dynamic response of the converter with lower conduction and turn-off losses. In Burdio et al. (2001), different fixed frequency control strategies are compared for identical values of input voltage and load for full-bridge SRC. It is observed that the asymmetrical clamped-mode (ACM) has low losses among the fixed frequency control schemes. However, control schemes like clamped-mode (CM) and asymmetrical duty-cycle mode (ADC) lead to the production of identical losses in the resonant converters.

The VF, SSOC and SSPSM control schemes are compared for full-bridge series converter in Youssef et al. (2005). The results show that the switch stress is highest for VF control scheme (3.93 p.u) and lowest for SSPSM (2.75 p.u). The range of conduction loss in different control scheme like VF, SSOC and SSPSM is 2.09 (p.u), 1.93 (p.u) and 1.75 (p.u) (Youssef et al., 2005; Salem et al., 2018).

The components size is maximum in the VF control scheme and moderates in the SSOC scheme while its value is minimum in the case of the SSPSM control scheme. The SSPSM control scheme is applicable to only full-bridge and the control schemes like VF and SSOC are applicable to both half-full-bridge topologies. In Youssef et al. (2005), different control schemes are applied to full-bridge series and parallel resonant converter and analyzed. It is observed that (SSPSM) has good dynamic performance as compared to other control schemes. A comparative study on different control schemes like phase-shift, frequency, and hybrid applicable to a series resonant converter used to charge EV battery using inductive method is discussed in Hayes and Egan (1999).

4. Bidirectional converters

4.1. Resonant converter based bidirectional EV charger

The bidirectional EV chargers based on resonant converter LLC and CLLC are discussed in this section. A SiC-based bidirectional EV charger includes two stages, with the first stage as boost type PFC and the second stage includes half-bridge LLC. It achieves an overall efficiency of 96% with a variable dc-link voltage control scheme. In addition, it is analyzed that the losses in both stages during the G2V mode of operation using the state–space model are discussed in Jiang et al. (2016).

The current stress on switches can be reduced with the help of full-bridge LLC (Musavi et al., 2013b). In a bidirectional LLC converter, the DC–AC converter is a buck converter in discharging mode. Therefore, the dc-link voltage must be greater than the peak grid voltage for its operation in grid-tied mode. The voltage compensation in reverse mode has been addressed in Li et al. (2020b) by increasing the dc-link voltage. Therefore, DC–AC inverter can be grid-connected. In an LLC converter, there are no blocking capacitors connected at the input of the LLC transformer in reverse mode. The unmatched conduction period can result in a non-zero voltage-second area, which may develop a dc bias current that will make the transformer saturate. This non-zero voltage is developed due to unbalanced conduction time which is caused by delay time difference of gate-driver circuit, uneven ON-state resistance of MOSFETs, and turn on and turn off time of MOSFETs. This can be avoided by the driver loop delay. It is the most important factor to remember when analyzing the dc bias current in the reverse mode in Zhang et al. (2020). A higher power density is achieved using CLLC converters which are connected in the delta at the primary side while three full-bridge connected in parallel on the secondary side. The advantage of this is that the current is equally shared in the resonant tank. In addition, high power density (155 W/in3) is achieved through a planer magnetic transformer that has a switching frequency of 500 kHz. It has an efficiency of 97% using GaN and SiC devices in Li et al. (2018a). The most preferred bidirectional converter is the CLLC (3-phase) resonant converter that operates up to a power level of 22 kW.

The current stress on switches can be reduced with the help of full-bridge LLC in Musavi et al. (2013b). In a bidirectional LLC converter, the DC–AC converter is a buck converter in discharging mode. Therefore, the dc-link voltage must be greater than the peak grid voltage for its operation in grid-tied mode. The voltage compensation in reverse mode has been addressed in Li et al. (2020b) by increasing the dc-link voltage. Therefore, DC–AC inverter can be grid-connected. In an LLC converter, there are no blocking capacitors connected at the input of the LLC transformer in reverse mode. The unmatched conduction period can result in a nonzero voltage-second area, which may develop dc bias current that will make the transformer saturate. This non-zero voltage is developed due to unbalanced conduction time which is caused by delay time difference of gate-driver circuit, uneven ON-state resistance of MOSFETs and turn on and turn off time of MOSFETs. This can be avoided by the driver loop delay. It is the most important factor to remember when analyzing the dc bias current in the reverse mode in Zhang et al. (2020). A higher power density is achieved using CLLC converters which is connected in the delta at the primary side while three full-bridge connected in parallel on the secondary side. The advantage of this is that the current is equally shared in the resonant tank. In addition, high power density (155 W/in $\hat{3}$) is achieved through a planer magnetic transformer that has a switching frequency of 500 kHz. It has an efficiency of 97% using GaN and SiC devices in Li et al. (2018a). The most preferred bidirectional converter is the CLLC (3-phase) resonant converter that operates up to a power level of 22 kW.

4.2. Control schemes of LLC and CLLC

In this section, control schemes for LLC and CLLC type converters are discussed. The control schemes are designed with an objective to transfer maximum power from the LLC or CLLC resonant converter to the EV battery with minimum switching losses. The main objective of the control scheme is to provide quick charging with a reduced value of settling time and with no overshoot or undershoot.

4.3. LLC

Different control schemes are proposed in the literature, like a phase-locked loop (PLL) and dual closed PLL for LLC resonant converter for EV battery charger (Asa et al., 2013; Colak et al., 2013). The PLL control scheme tracks the resonant frequency and ensures that a soft-switching action is maintained. In the control scheme discussed in Asa et al. (2013), the battery is charged in CC and CV modes. However, the performance of the resonant converters with CC and CV modes of operation is not included in Asa et al. (2013). The dual closed-loop control scheme includes two control loops which are CC-CV and PLL control loops. The CC-CV control loop is used in the ac–dc converter while the PLL control loop is used to track the resonant frequency in the LLC converter. It is observed that there is a smooth transient from CC mode to CV mode of battery charging (Colak et al., 2013).

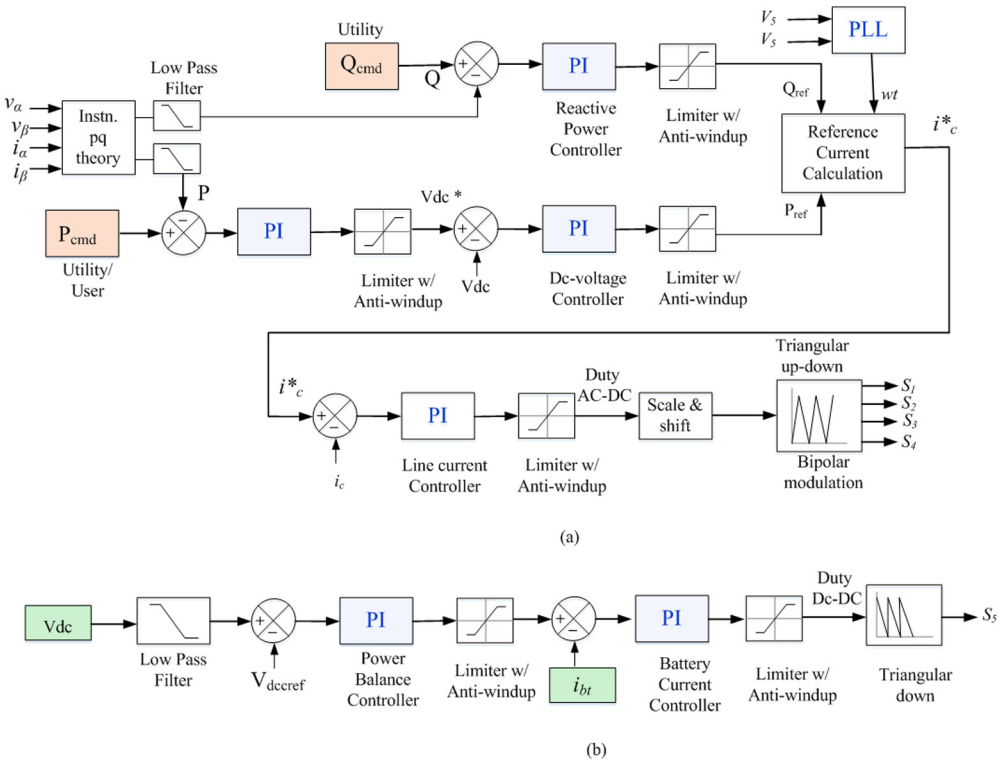

Fig. 17. (a) Control for ac–dc (b) control for dc–dc.

4.4. CLLC

The various control schemes used for CLLC topology are discussed in the literature. The maximum efficiency tracking scheme is proposed in Liu et al. (2016). However, it does not provide any experimental evidence to back up such a claim. The design details of the CLLC converter are discussed in Lv et al. (2015). It lacks in synchronous rectification on the secondary side, which will cause large conduction losses. The above-mentioned limitation of synchronous rectification on the secondary side is resolved in Zou et al. (2017b). In this scheme, the battery is charged in CC and CV mode with the help of two-control loops, which include a linear proportional plus integral (PI) controller implemented in the digital domain. It is observed that the settling time (T_S) of the controller is within 30 ms during step-up and step-down operation of the load. The settling time (T_S) is further reduced by using a sliding mode control scheme for a bidirectional CLLC resonant converter, which is suggested in Zou et al. (2019). The magnitude of the steady-state error is less than 0.5%, and the settling time (T_S) is 1 ms. However, using the conventional PI control strategy, the settling time value is observed to be 0.9 ms. The overall efficiency of the CLLC converter is 97%.

5. Control scheme for the exchange of active and reactive power in V2G mode of operation

The unidirectional EV charger has the limitation that the power flows from grid to vehicle only. Moreover, there is an option of using the battery's stored energy. Since EV is parked more than 85% of a lifetime, stored energy in EV batteries can be utilized to support grid or to provide ancillary services. It is possible to inject energy in the utility or main grid from the EV batteries, using a bidirectional converter.

The bidirectional power flow is possible in vehicle-to-grid (V2G), vehicle-to-home (V2H), home-to-vehicle (H2V), and vehicle-to-Vehicle (V2V) modes. In V2G mode, the EV charger regulates the voltage and frequency of the grid. The stored energy can provide ancillary services like harmonic compensation, reactive power support. In the V2G mode of operation, the exchange active and reactive powers with the grid can be controlled using various control schemes discussed in Tanaka et al. (2013), Pinto et al. (2013), Ferreira et al. (2011) and Kisacikoglu et al. (2014). The control scheme used for the injection of active and reactive power in V2G mode operation discussed in Kisacikoglu et al. (2014) is shown in Fig. 17 shows the control scheme of the AC–DC converter used to inject active, P, and reactive power, Q. The active and reactive power to be injected is controlled by using linear PI controllers. The PI controllers minimize the difference between the actual and desired value of active P_{cmd} and reactive power Q_{cmd} The output of the PI controller used to control P is supplied to the DC-link voltage controller. The output of PLL, reactive power controller, DC-link voltage controller is used to synthesizing the reference value of inductor current. By minimizing the difference between the actual ic and reference value i*c of the inductor current, the desired value of active and reactive powers (P_{cmd}, Q_{cmd}) to be injected in V2G mode can be achieved. The control scheme of the DC–DC converter used to supply the energy from the battery to the grid in the V2G mode of operation is shown in Fig. 3b. The battery voltage is regulated with the help of a voltage controller. The output of voltage controller act as the reference for the current controller. By minimizing the difference between the actual value of battery current and desired value battery current, the desired value of active and reactive power to be supplied by the battery to the grid can be controlled. A comparison table between different control schemes for active and reactive power exchange is given in Table 5.

6. Battery charging modes

There are various types of battery charging strategies. The battery charging strategy refers to the shape and magnitude of

Table 5
Comparison of various control schemes.

Modulation Control Types	Conduction loss (Youssef et al., 2005; Salem et al., 2018)	Converter control		V2G Control
		LLC (Asa et al., 2013; Colak et al., 2013)	CLLC (Liu et al., 2016; Lv et al., 2015; Zou et al., 2019)	P and Q (Tanaka et al., 2013; Pinto et al., 2013; Ferreira et al., 2011; Kisacikoglu et al., 2014)
Variable frequency	2.09 (p.u), size of components is maximum	Variable-DC link	Maximum-efficiency (Ts)-	Two separate controllers scheme
Self-sustained oscillation (SSOC)	1.93 (p.u), size of components is moderate	Dual-Closed loop scheme	Proportional–integral (PI)-(Ts)-30 ms	Uniform controller scheme
Self-sustained phase oscillation (SSPSM)	1.75 (p.u), size of components is minimum	Dual-Closed loop scheme	Sliding mode- (Ts)- 9 ms	Unified controller scheme

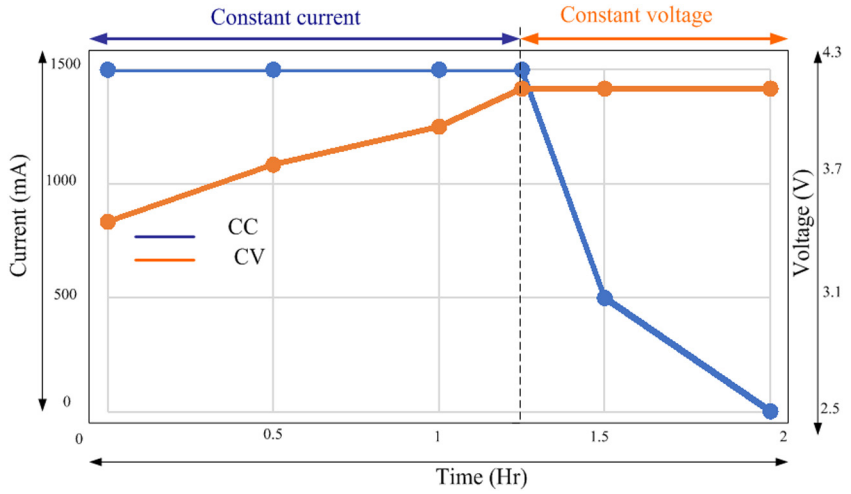

Fig. 18. Battery charging modes.

the current/voltage required for charging a battery. The basic battery charging strategies adopted in EV chargers are Constant Current (CC), and Constant Voltage (CV) as shown in Fig. 18. The CC and CV modes of charging operations of batteries are discussed in Collin et al. (2019). A brief introduction of these modes is as follows:

1. Constant Current Charging Method: In this method of charging, the battery is charged in such a way that the charging current remains constant. This method is applied when the battery voltage is far below the nominal value of its terminal voltage. Drawback — The CC mode of battery charging may cause overheating and damage the battery. This leads to a reduction in the useful life span of the battery.
2. Constant Voltage Charging Method: In this mode of charging, the battery is charged in such a way that charging across the battery terminals remains constant. The charging voltage is maintained at a slightly higher value than the nominal value of battery voltage. During the charging process, the maximum voltage should be applied to a certain type of battery while charging current slowly decreases as the full battery charge approaches.
3. The CC and CV modes of operation are shown in Fig. 18. This figure shows that during the CC mode of operation, the charging current is maintained at a constant value. The value of the battery terminal voltage rises linearly. Now, when the value of terminal voltage's the value becomes almost equal to 80% of its nominal value, the transition from CC mode to CV takes place. Now the battery voltage remains constant, and the charging current goes on decreasing. When the battery becomes full, the charging current supplied to the battery is reduced to zero.

Drawback — It takes a long time to charge battery fully.

7. Comparison's of existing topologies

There are three configurations of LLC Converter which are compared in Table 6. It is observed that half-bridge configuration has a lesser number of devices as compared to full-bridge and three-level LLC. Half-bridge configuration is simple to implement. However, it has higher stress on switches and produces ripples of large magnitude in output current. To resolve this issue, a full-bridge LLC configuration is used. It has high reliability and low EMI. However, the cost of LLC based resonant converter is high and difficult to design. The TL-LLC configuration is costlier as compared to other configurations. It is suitable for high power applications as voltage stress is half of the supply.

Table 7 shows a comparison of unidirectional converters of 1 kW, 1.5 kW and 3.3 kW. While bidirectional converter SR, LLC, CLLC is of 3.5 kW, 6.6 kW wattage is compared in Table 7. In Wang et al. (2013) the first stage of this converter is interleaved boost converter and the second stage has a full-bridge LLC converter. It has an efficiency of 95.4%. The DC-link capacitor is bulky and has high current flows during starting which causes the temperature to rise and reduces the charger life. However, details of the first stage performance is not discussed sufficiently in the literature. A full-bridge LLC converter with variable dc-link is preferred in the second stage. The maximum efficiency of the converter is tracked (Wang et al., 2014a).

A hybrid converter formed by combining SRC plus LLC resonant tank circuit is discussed in Wang (2015) for the second stage. It has an efficiency of 96.8%. The disadvantage is that number of transformers increases to two and resonant components to five. For a charger having a power rating of 1.5 kW wattage

Table 6
Comparison table of LLC topologies (Zeng et al., 2020).

Topology	L	C	D	S	TX	Total devices	Merits	Demerits
Half-bridge LLC	2	2	2	2	1	9	• The primary side of the transformer has low voltage stress. • Simple structure and low cost. • Continuous current on the primary side so full use magnetic core and magnetic bias eliminated	• Higher current stress on switches and primary side of the transformer • A higher current ripple that causes voltage oscillations and spikes To fit for a wide range of input voltage, the magnetizing inductor must be small. The high value of magnetizing inductance will increase conduction and hysteresis losses which results in reduction in converter efficiency. • If only high-voltage-tolerance power devices are used, conduction losses in the low-voltage condition will increase dramatically, lowering the converter's overall efficiency for the wide range input voltage case.
Full-bridge- LLC	2	2	2	4	1	11	• Small ripple • Low EMI • High reliability • Voltage and current Stress are lower	• Design is complex • Cost is high as more number gate driver required • Ripple in the current of the secondary side of the transformer is high that can lead to voltage spikes and oscillations
Three Level (TL)-LLC	2	3	4	4	1	14	• It is suited for high power settings because the voltage stress on the switches is decreased to half of the input voltage. • Harmonic content is low in output voltage	Complex design as more components.

is discussed in Shahzad et al. (2015). The first stage is a PWM rectifier with boost PFC, while for the second stage, a half-bridge LLC converter that charges a lithium battery of 320–420 V. Here power factor is improved with hysteresis current control. The author has not discussed the efficiency of the converter and losses calculation. The unidirectional charger of power rating of 3.3 kW is discussed in Deng et al. (2013). The charger is used to charge lithium-ion of 250–400 V. The second stage of the charger has a full-bridge LLC with the highest efficiency of 98.2%. In the first stage, the SEPIC PFC converter is implemented in Wang et al. (2014b) and full-bridge LLC for the second stage. In addition, the new control method is proposed to track the maximum point in the LLC converter. However, details of THD, the efficiency of the first stage and its designing steps are not included. From Table 7, it is observed that by using variable dc-link voltage control scheme, maximum efficiency of LLC converter can be tracked. In addition, the LLC topology has a lower value of L_m as compared to the hybrid combination (SRC+ LLC) that lowers the circulating current.

Now in Table 7, a comparison of bidirectional converters having power ratings of 3.5 kW and 6.6 kW is included. A turn off-delay in bidirectional Series resonant converter having a power rating of 3.5 kW is implemented along with its proposed configuration that will expand the voltage gain of the converter (Yang et al., 2020). The performance details of the first stage and control scheme and the addition of an auxiliary inductor are few negative impacts.

In Li et al. (2018b), for bidirectional LLC converter of power rating of 6.6 kW has an efficiency of 96.37% in charging mode. Its efficiency is 96.87% @3 kW in discharging mode. For $L_r = 8.5$ uF, $C_r = 33$ nF and $L_m = 24$ uH and resonant frequency $f_r = 300$ kHz and that charges a battery of lithium-ion with voltage range of 240–420 V. The limitation is that an additional non-isolated DC–DC converter is added between two stages that adds extra cost and size. In Li et al. (2021b) and Li et al. (2020b), implemented totem pole bridgeless for the first stage and second stage is full-bridge LLC converter. Here, both converters are having different control schemes. The highest power density of the charger is 56 W/in3 in Li et al. (2020b). A full-bridge CLLC converter is referred to as the second stage in Li et al. (2018c) with the efficiency of 96% and power density −37 W/in3. The limitation is that the number of resonant components increases to 4 and transformers to 2. Moreover, the details of the performance of the first stage are not included.

The main difference between unidirectional (LLC, SRC+ LLC) and bidirectional (SRC, LLC and CLLC) EV chargers converters is the direction of flow of power, type of converter used in the first stage and second stage, switching frequency and battery voltage. For unidirectional converter in the first stage (AC–DC) interleaved boost, rectifier boost and SEPIC with PFC are preferred. In the second stage (DC–DC), a half-bridge, full-bridge-LLC or hybrid converter can be preferred. With resonant frequency $f_r = 200$ kHz and battery voltage around 320V-400V for (1 kW, 1.5 kW) and 250 V, 100–400 V (3.3 kW). Furthermore, variable dc-link and maximum point tracking point approaches can be used to extract the maximum efficiency of the second stage converter. In a bidirectional converter, the first stage (AC–DC) is of Totem pole bridgeless or interleaved totem bridgeless pole type. For the second stage (DC–DC) full-bridge LLC, SRC and CLLC are preferred. With $f_r = 300$ kHz, the battery voltage varies from 200 V, 240V–420 V, 500 V. In discharging mode, the DC–AC converter is in buck mode. For (V2G) mode, the dc-link voltage must be higher than the peak grid voltage. This is accomplished via a voltage compensation approach that raises the dc-link voltage. It is observed that the value of L_m is high in series resonant converter as compared to LLC converter (Siebke et al., 2019).

7.1. List of companies that install EV charging stations

The list of companies that install EV chargers is represented in the appendix. There are 4 major companies which are Pod

Table 7
Comparison table of unidirectional and bidirectional EV charger topologies.

Ref. no	Wattage (kW)	Efficiency (%)	Lr (uH)	Cr (nF)	Lm (uH)	Fr (kHz)	X	Battery voltage (V)	Total no. of resonant components (Lr+ Lm+ Cr) and X	Advantages	Disadvantage
Unidirectional											
Wang et al. (2013)	1	95.4	62.51	10	160	200	1	320-420 lithium ion	1 + 1 + 1 = 3, 1	1. 1st Interleaved boost. 2. 2nd Full bridge LLC. 3. Complete design guideless for both stages	1. There is no details of THD performance of first stage. 2. For second stage design steps, losses calculations
Wang et al. (2014a)	1	2.1% at heaviest load and 9.1% in light load	31.7	20	107.6	200	1	320- 420	1 + 1 + 1 = 3, 1	1. 1st 2. 2nd Full bridge LLC. 3. By means of variable dc-link method maximum efficiency of LLC converter is achieved.	1. There is no details of THD performance of first stage. 2. For second stage design steps, losses calculations
Wang (2015)	1	96.80%	Lr1- 63.4, Lr2- 31.7	Cr1- 10, Cr2- 20	80	200	2	–	2 + 1 + 2 = 5, 2	1 1st 2. 2nd Hybrid (SRC+ LLC) 3. Reduces the turn 0ff current, circulating current and peak current of the MOSFET.	1. The negative impacts that the number of transformer increases (2), resonant component increases (5). 2. There is no details of THD performance of first stage.
Shahzad et al. (2015)	1.5	–	33.42	18.95	133.68	200	1	320-420	1 + 1 + 1 = 3, 1	1. 1st Rectifier and boost PFC 2. 2nd Half bridge LLC 3. First stage boost converter Power factor is improved with hysteresis control and second stage LLC converter	1. Absence of efficiency and losses calculation. 2. Half bridge LLC converter is used.
Deng et al. (2013)	3.3	Peak- 98.2%	26.25	40.33	133.1	150	1	250-400, Lithium ion	1 + 1 + 1 = 3, 1	1. 1st 2. 2nd Full bridge LLC 3. The worst case operating point is used for design purpose and worst case condition for primary side (ZVS) are analyzed.	1. No analysis of core loss, switching and conduction loss 2. For wide voltage gain variations. it is necessary to vary fs widely with respect to voltage gain. This will reduce the efficiency and undermines the soft switching 3. There is no details of THD performance of first stage.
Wang et al. (2014b)	3.3	Efficiency Improvement 4.4% at heaviest 16.5% lightest load situation	31.7	20	107.6	200	1	100-400, Lithium ion	1 + 1 + 1 = 3, 1	1. 1st SEPIC PFC 2. 2nd Full bridge LLC 3. The worst case operating point is used for design purpose and worst case condition for primary side (ZVS) are analyzed.	1. No analysis of core loss, switching and conduction loss 2. For wide voltage gain variations. it is necessary to vary fs widely with respect to voltage gain. This will reduce the efficiency and undermines the soft switching 3. There is no details of THD performance of first stage.
Bidirectional											
Yang et al. (2020)	3.5	97.90	36	71	500-La-500	–	1	250- 400	1 + 2 + 1 = 3, 1	1. 1st 2. 2nd Full bridge TFD-BSR 3. Proposed a new configuration that expands the voltage gain of series converter	1. There is no details of THD performance of first stage and control strategy. 2. Additional auxiliary inductor.
Li et al. (2018b)	6.6	96.37 @6.6 kW in charging mode 96.87 @3 kW discharging	8.5	33	24	300	1	240-420	1 + 1 + 1 = 3, 1	1. 1st Totem pole bridgeless PFC 2. 2nd Full bridge LLC 3. Proposes a OBC with first interleaved totem bridgeless PFC and mode — switched DC–DC converter.	1. Additional non-isolated DC–DC converter between the first stage and second stage.
Li et al. (2021b)	6.6	95.5 @6.6 kW charging mode, 96.6 @3.3 kW discharging mode, 97.80, power density- 36.3 W/in3	12.8	49.9	22	300	1	240-420	1 + 1 + 1 = 3, 1	1. 1st Totem pole bridgeless PFC 2. 2nd Full bridge LLC	1. Design steps of LLC converter is absent and loses calculation. 2. Control scheme along with mathematical models to calculate the SR on-time online. In reverse mode, the LLC's transformer dc bias is examined.
Li et al. (2020b)	6.6	96 @6.6 kW in both charging mode and dis-charging mode. power density −56 W/in3	16.51	75	17	30	1	200-500	1 + 1 + 1 = 3, 1	1. 1st-Totem pole bridgeless PFC, 2. 2nd-Full bridge LLC 3. In reverse mode Voltage compensation controlled by regulating dc-link voltage. and digital adaptive SR driving scheme was proposed based on LLC primary driver signals	1. Two switches are added in first stage. 2. (SR) scheme only considers the switching frequency and neglects the load variations. 3. Absence of blocking capacitor in LLC transformer input in reverse mode which may induce transformer saturation 4. No mathematical analysis for SR calculation on time
Li et al. (2018c)	6.6	96% power density −37 W/in3	Lr1-3 (primary) Lr2- 1.5 (secondary)	Cr1-34 (primary) Cr2-68 (secondary)	–	500	2	250-450	2 + 0 + 2 = 4, 2	1. 1st-Totem pole bridgeless PFC 2. 2nd-full bridge CLLC 3. A control strategy is proposed for combined two-stages.	1. Design steps of CLLC converter is absent. 2. There is no details of THD performance of first stage. 3. More number resonant components and two transformer

point, ABB, eo and efarady. The Ev chargers are provided for home, commercial and workplace. In the first category, Pod point company has a solo charger model of 3.6 kW, 7 kW or 22 kW for home charging. There are three different types of chargers available for commercial purpose. these are Solo chargers (up to 22 kW), Twin charger (up to 22 kW) and Media Charger (up to 7 kW) while for workplace, the EV charger that can be installed are solo chargers or twin charger up to 22 kW. In the second category, ABB company two types one for home charging AC destination (3 to 22 kW) and the other for DC destination (11 to 24 kW). DC destination (11 to 24 kW), DC Fast (50 to 180 kW) and DC high power for commercial point. The DC Fast charger is further classified as city charger point, retail shopping centers and highway corridors and fleet. Tera 124 charger can charge one

EV vehicle up to 180 kW while two EVs upto a power rating of 60 kW. Terra 184 can charge single EV up to 180 kW and two EVs upto a power rating of 80 kW. The Terra is capable of charging up to 350 kW with a 500 A current and simultaneously two EVs can be charged till 175 kW with a 375 A current. The connectors required for DC destination and DC fast are CCS1, CSS2 and CHademo. For high power ratings, the Liquid-cooled feature in CCS1, CSS2 and CHademo connector are required. The third company eo has three different options for charging. These are EO mini, EO Mini Pro of wattage 3.6 kW and 7 kW that needs type 1 or type 2 connector. EO Mini Pro has a smartphone-controlled that tracks energy usage and charging schedules. EO basic of wattage 3.6 kW, 7 kW, 11 kW and 227 kW with an additional feature of high-speed charging can lock the socket that restricts others to charge. EO Genius charger can be used for commercial and workplace charging stations that can charge up to 22 kW. efardy company has three types of in-home charger which are Indra smart pro (up to 7 kW), ease (22 kW) and ANDERSON (22 kW). Ease and ANDERSON includes a type 2 connector type 2 and type 1 for Indra smart pro. For Commercial category, TRITIUM (25.75 kW), ALFEN (3.7kW–22 kW), ETREL INCH PRO (7.4 kW, 22 kW) and ETREL INCH DUO (22 kW) are used. For workplace charging station, efarday TRITIUM (25.75 kW), ALFEN (3.7kW–22 kW) and ease (22 kW) are used.

8. Challenges and solutions

The bidirectional converters have more benefits like (ancillary service, operating in different modes V2G,V2H and V2V) as compared to unidirectional converters. However, bidirectional converters include more power switches which in turn increases the cost. In addition, it increases the switching loss and reduces the overall efficiency and power density. Challenges associated with bidirectional converters are depicted in pictorial form, as shown in Fig. 19. The EV chargers are commonly designed using Si-based devices which are operated below the switching frequency of 100 kHz. The operation above this frequency range may lead to excessive switching and conduction losses and may cause thermal breakdown of the device. The performance of a resonant converter is largely affected by a resonant frequency which plays an important role. If the selected value of resonant frequency is high, it will result in a lower value of Lm magnetizing inductance which increases the circulating currents. If the resonant frequency has a lower value, it causes a smaller value of Zr and fs, which reduces the power density of the converter. The further challenge is related to the converter operating region. To ensure zero voltage switching, the resonant converter should be operated at the resonant frequency. Efficiency is changed when switching frequency shifts from the resonant frequency. As discussed above, the operating frequency of silicon (Si)-based chargers is 100 kHz which leads to a huge footprint of passive components. It is a viable approach for achieving high power density by drastically reducing the size of the passive components. In the case of Si-based converters, the efficiency drops significantly when the switching frequency is increased. It is due to an increment in switching losses and conduction loss (considering the positive junction temperature coefficient), ac winding loss, and core loss of the magnetic components. And the last challenge is the compensation network. In LLC-based resonant converters, the resonant tank is unsymmetrical in nature, which may cause unequal sharing of current in the resonant tank.

The possible solutions to the above-mentioned challenges are listed below

1. The inclusion of wide-band gap devices in resonant converters increases efficiency and power density. These devices have a significantly higher figure of merit (FOM), which are able to significantly improve efficiency and power density. The silicon carbide (SiC) devices are able to operate at hundreds of thousands of frequencies to get a higher power density. The operation at a higher switching frequency leads to a reduction in the size of passive components. The SiC-based MOSFETs have a lower ON state resistance than Si-based MOSFETs for the same rating of conduction current. Therefore, the SiC-based MOSFETs have reduced conduction losses and higher efficiency. Therefore, these devices are considered a good option on-board chargers (OBCs).
   Despite several advantages of SiC and GaN devices, there are a few challenges associated with these devices like high cost, complex design of gate drivers, and complex design of protection against EMI. Further, the efficiency of GaN and SiC drops by 4% when the operating temperature is increased from 50 degrees to 150 degrees.
2. It is necessary to design the magnetic components in an optimal fashion. The approach suggested in the literature is used to design resonant converters using large gap transformers (Finkenzeller et al., 2020). Another possible solution is to use a planer transformer in Li et al. (2018a).
3. The soft switching region can be extended with the help of modulation schemes and the selection of control schemes that tracks the resonant frequency in Wang (2015).
4. The resonant converters should be operated high values of switching frequencies with an objective to reduce the size of the passive components in Li et al. (2018a).
5. The challenges associated with the compensation network are overcome by proper selection of reactive components included in two-element, three-element, and multi-element resonant converter, making tank circuit to be symmetrical like CLLC type of tank circuit and by using multiple stages of tank circuit in Beiranvand et al. (2011), Wu et al. (2016) and Shang and Wang (2018), Wang et al. (2019).

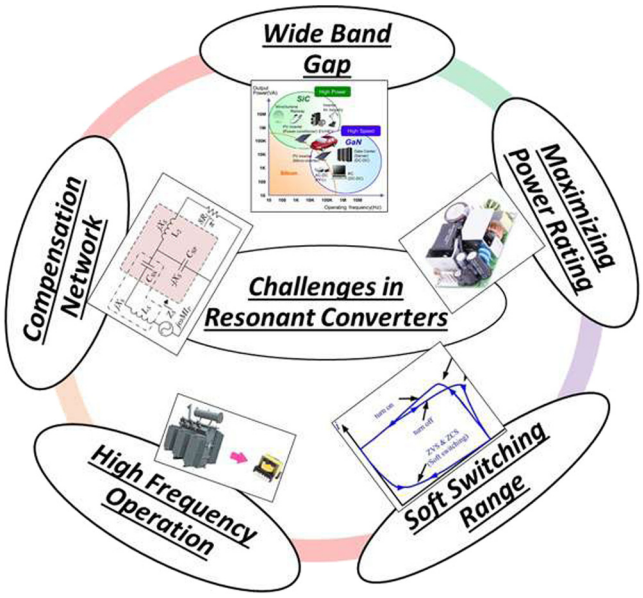

Fig. 19. Challenges in resonant converter.

9. Future research area

The main objective for developing an EV charger, including resonant power converter, is to achieve high efficiency, high

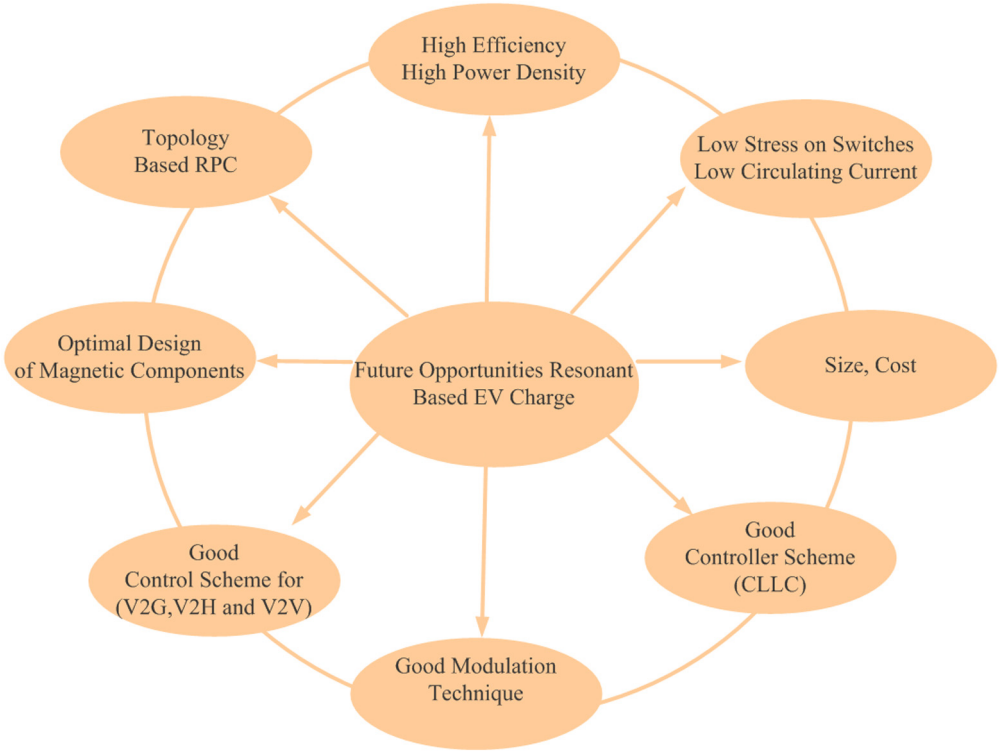

Fig. 20. Future research area.

power density, compact size, and low cost. Based on these objectives, the section related to future research highlights the opportunities for the resonant converters in the near future. The scope of future research related to the domain of resonant converter chargers is shown in Fig. 20 . The single and two-stage resonant converters, which have high reliability and high-power density, are being developed. Moreover, it is desired that the resonant converter-based topology should be compact in size, low cost, and reduced circulating current to minimize the losses. The conventional modulation schemes used in EV chargers suffer from the limitations like higher conduction losses, the large physical size of components, and more voltage stress on switches. This can be improved by devising new modulation schemes. There is a need to develop fast chargers for EVs, which reduces the charging time of electric vehicles. Further, the developed EV charger should ensure a smooth transition from constant-current (CC) to constant-voltage (CV) mode with reduced settling time and minimum overshoot value. In addition, the operation of the resonant converter should be stable against the parameter variation and external disturbances. To fulfill these objectives, efficient and robust control schemes are required to be developed for the resonant converter-based EV chargers (LLC or CLLC). To enhance the system's reliability and provide the ancillary services like minimization of frequency deviation, voltage difference, harmonic compensation, and reactive power support, efficient bidirectional resonant converters are required to be developed. These converters enable the operation of the system in various operating modes like V2G, V2H, and V2V and provide above mentioned ancillary services to the system. The control schemes which can ensure efficient exchange of active and reactive power and ancillary services to the system are needed to be investigated. Further, the optimal design of magnetic components is necessary to reduce the physical size of components and cost. This leads to an improvement in the performance of the converter. From the above-mentioned discussion, it can be concluded that there is a need to develop resonant converter-based EV chargers, which will resolve above-mentioned limitations.

10. Conclusion

This paper gives, a state-of-the-art literature review on resonant converters used in EV charger applications. In this classification of resonant converter, the guidelines for selecting of various resonant converter-based two-stage EV chargers are discussed. From the various resonant converter-based topologies discussed in the literature, it is observed that the CLLC resonant converter has good efficiency. However, the cost of implementation is higher, and the circuits become more complex for analysis due to the inclusion of more reactive elements. In addition, the various modulation schemes used for resonant converters-based chargers like variable frequency, fixed frequency, self-sustained oscillation, and self-sustained phase-shift modulation. Among various modulation schemes used with resonant converters-based chargers reported in the literature, the SSPSM modulation scheme is considered good a candidate. The implementation of this modulation scheme leads to lower conduction losses and a reduction in the physical size of components. Further, the controller in the case of the LLC-CLLC resonant converter is discussed in detail. The sliding mode controller has a smaller steady error (< 0.5%) and reduces the value of settling time, thus improving the transient response of the system. The controller used for active power (P) and reactive power (Q) injection in the V2G mode of operation is elaborated in detail. For the exchange of active and reactive power between EV and grid, the unified controller scheme makes the dynamic performance of the system to be faster. The use of SiC and GaN devices in resonant converter-based topologies leads to improvement in efficiency and power density of the chargers. The associated challenges with resonant converter-based EV charges are highlighted, and their future scope is also included.

Declaration of competing interest

The authors declare that they have no known competing financial interests or personal relationships that could have appeared to influence the work reported in this paper.

Acknowledgments

This publication, is made possible by NPRP grant #[13S-0108-2000228] from the Qatar National Research Fund (a member of Qatar Foundation). The statements made herein are solely the responsibility of the authors. The APC for the article is funded by the Qatar National Library, Doha, Qatar.

Appendix

See Table 8.

Table 8
List of commercial companies that install EV charging stations.

Company name	Home charging	Commercial charging	Workplace charging
Pod point (Pod-Point, 2021)	Solo charger-3. 6 kW, 7 kW or 22 kW Connector (Universal socket or tethered version)	1. Solo charger-(up to 22 kW) 2. Twin charger-(up to 22 kW) 3. Media Charger (up to 7 kW) Connector –	1. Solo charger-(up to 22 kW) 2. Twin charger-(up to 22 kW) Connector –
ABB (ABB, 2021)	1. AC Destination -(3 to 22 kW) (Terra AC wallbox) (3to 22 kW) Connector- (socket type 2) 2. DC destination- (Terra DC wallbox) (11 to 24 kW) Connector CCS1,CCS2 and CHademo	1. DC destination-(11 to 24 kW) (Terra DC wallbox) (11 to 24 kW) Connector CCS1,CCS2 and CHademo 2. DC Fast -(50 to 180 kW) (1) City charger Points Terra fast chargers- Terra 54 (50 kW) Terra 94 (94 kW) (2) Retail/Shopping center (Terra 124) for one EV upto 120 kW For two EVs upto 60 kW (3) Highway corridors and Fleet (Terra 184) for one EV upto 180 kW For two EVs upto 90 kW Connector CCS-1: 200 A; CHAdeMO: 200 A (4) DC High Power (Terra high power gen III) High power charging at up to 350 kW and 500 A at either charge post. Simultaneous charging at up to 175 kW and 375 A at both charge posts. Connector CCS1/CCS2 (liquid cooled) CHAdeMO	–
eo (Charging, 2021)	1. EO Mini (3. 6 kW,7 kW) Connector Universal socket, Type 1 or Type 2 Tethered (Model dependent) 1. EO Mini Pro2 (3. 6 kW, 7 kW) Connector-Universal socket, Type 1 or Type 2 Tethered (Model dependent) 3. EO Basic (3. 6 kW, 7 kW, 11 kW, 22 kW) Connector Universal socket, Type 1 or Type 2 Tethered (Model dependent)	1 EO Genius chargers (up to 22 kW) 1. Fleet charging, Car Parks and Destination Connector –	2 EO Genius chargers (up to 22 kW) Connector –
efaraday (Efaraday, 2021)	1. Indra Smart Pro Max. output power: 7. 4 kW.	1. TRITIUM 25–75 kW	1. TRITIUM 25–75 kW

(continued on next page)

Table 8 (*continued*).

Company name	Home charging	Commercial charging	Workplace charging
	Connector Type 2 socket, Type 1 or Type 2 tethered cable 2. easee up to 22 kW Connector Type 2 connector 3. ANDERSEN up to 22 kW Connector Type 2 connector	Connector CCS1, CCS2 and/or CHAdeMO 2. ALFEN 3. 7-22 kW Connector Type −2 3. ETREL INCH PRO 7. 4 kW (1 × 32 A), 22 kW (3 × 32 A) Connector Type-2 3. ETREL INCH Duo 2 × 22 kW (3 × 32 A per connector) adjustable	Connector CCS1, CCS2 and/or CHAdeMO 2. ALFEN 3. 7-22 kW Connector Type −2 3. easee up to 22 kW Connector Type 2 connector

References

ABB, EV charging solutions. URL https://new.abb.com/ev-charging. (Accessed 08 Aug. 2021).

Adragna, C., De Simone, S., Spini, C., 2008. A design methodology for LLC resonant converters based on inspection of resonant tank currents. In: 2008 Twenty-Third Annual IEEE Applied Power Electronics Conference and Exposition. IEEE, pp. 1361–1367.

Asa, E., Çolak, K., Czarkowski, D., de León, F., Sefa, I., 2013. Pll control technique of LLC resonant converter for EVs battery charger. In: 4th International Conference on Power Engineering, Energy and Electrical Drives. pp. 1382–1386. http://dx.doi.org/10.1109/PowerEng.2013.6635816.

Bae, S., Gros, S., Kulcsár, B., 2021. Can AI abuse personal information in an EV fast-charging market? IEEE Trans. Intell. Transp. Syst. 1–11.

Bai, C., Han, B., Kwon, B.-H., Kim, M., 2020. Highly efficient bidirectional series-resonant DC/DC converter over wide range of battery voltages. IEEE Trans. Power Electron. 35 (4), 3636–3650. http://dx.doi.org/10.1109/TPEL.2019.2933408.

Batarseh, I., 1994. Resonant converter topologies with three and four energy storage elements. IEEE Trans. Power Electron. 9 (1), 64–73. http://dx.doi.org/10.1109/63.285495.

Beiranvand, R., Zolghadri, M.R., Rashidian, B., Alavi, S.M.H., 2011. Optimizing the LLC–LC resonant converter topology for wide-output-voltage and wide-output-load applications. IEEE Trans. Power Electron. 26 (11), 3192–3204.

Burdio, J., Canales, F., Barbosa, P.M., Lee, F.C., 2001. Comparison study of fixed-frequency control strategies for ZVS DC/DC series resonant converters. In: 2001 IEEE 32nd Annual Power Electronics Specialists Conference (IEEE Cat. No. 01CH37230), Vol. 1. IEEE, pp. 427–432.

Charging, E., Smart electric vehicles charging. URL https://www.eocharging.com/. (Accessed 08 Aug. 2021).

Colak, K., Asa, E., Czarkowski, D., 2013. Dual closed loop control of LLC resonant converter for EV battery charger. In: 2013 International Conference on Renewable Energy Research and Applications. ICRERA, pp. 811–815. http://dx.doi.org/10.1109/ICRERA.2013.6749864.

Collin, R., Miao, Y., Yokochi, A., Enjeti, P., Von Jouanne, A., 2019. Advanced electric vehicle fast-charging technologies. Energies 12 (10), 1839.

Deng, J., Li, S., Hu, S., Mi, C.C., Ma, R., 2013. Design methodology of LLC resonant converters for electric vehicle battery chargers. IEEE Trans. Veh. Technol. 63 (4), 1581–1592.

Duerbaum, T., 1998. First harmonic approximation including design constraints. In: INTELEC-Twentieth International Telecommunications Energy Conference (Cat. No. 98CH36263). IEEE, pp. 321–328.

Efaraday, EV charging solutions. URL https://efaraday.co.uk/. (Accessed 08 Aug. 2021).

Fang, Z., Cai, T., Duan, S., Chen, C., 2015. Optimal design methodology for LLC resonant converter in battery charging applications based on time-weighted average efficiency. IEEE Trans. Power Electron. 30 (10), 5469–5483.

Fang, X., Hu, H., Shen, Z.J., Batarseh, I., 2011a. Operation mode analysis and peak gain approximation of the LLC resonant converter. IEEE Trans. Power Electron. 27 (4), 1985–1995.

Fang, X., Hu, H., Shen, Z.J., Batarseh, I., 2011b. Operation mode analysis and peak gain approximation of the LLC resonant converter. IEEE Trans. Power Electron. 27 (4), 1985–1995.

Fang, X., Hu, H., Shen, J., Batarseh, I., 2012. An optimal design of the LLC resonant converter based on peak gain estimation. In: 2012 Twenty-Seventh Annual IEEE Applied Power Electronics Conference and Exposition. APEC, IEEE, pp. 1286–1291.

Ferreira, R.J., Miranda, L.M., Araújo, R.E., Lopes, J.a.P., 2011. A new bi-directional charger for vehicle-to-grid integration. In: 2011 2nd IEEE PES International Conference and Exhibition on Innovative Smart Grid Technologies. IEEE, pp. 1–5.

Finkenzeller, M., Poebl, M., Komma, T., 2020. A new approach of resonant converter using large air gap transformer. In: 2020 22nd European Conference on Power Electronics and Applications. EPE'20 ECCE Europe, pp. P.1–P.8. http://dx.doi.org/10.23919/EPE20ECCEEurope43536.2020.9215723.

Hayes, J.G., Egan, M.G., 1999. A comparative study of phase-shift, frequency, and hybrid control of the series resonant converter supplying the electric vehicle inductive charging interface. In: APEC'99. Fourteenth Annual Applied Power Electronics Conference and Exposition. 1999 Conference Proceedings (Cat. No. 99CH36285), Vol. 1. IEEE, pp. 450–457.

He, P., Khaligh, A., 2016. Comprehensive analyses and comparison of 1 kw isolated DC–DC converters for bidirectional EV charging systems. IEEE Trans. Transp. Electrif. 3 (1), 147–156.

Huang, D., Lee, F.C., Fu, D., 2011. Classification and selection methodology for multi-element resonant converters. In: 2011 Twenty-Sixth Annual IEEE Applied Power Electronics Conference and Exposition. APEC. pp. 558–565.

Jiang, C., Lei, B., Teng, H., Bai, H.K., 2016. The power-loss analysis and efficiency maximization of a silicon-carbide MOSFET based three-phase 10kW bi-directional EV charger using variable-DC-bus control. In: 2016 IEEE Energy Conversion Congress and Exposition. ECCE, pp. 1–6. http://dx.doi.org/10.1109/ECCE.2016.7855508.

Jing, H., Jia, F., Liu, Z., 2018. Multi-objective optimal control allocation for an over-actuated electric vehicle. IEEE Access 6, 4824–4833.

Khaligh, A., D'Antonio, M., 2019. Global trends in high-power on-board chargers for electric vehicles. IEEE Trans. Veh. Technol. 68 (4), 3306–3324.

Kim, M., Jeong, H., Han, B., Choi, S., 2018. New parallel loaded resonant converter with wide output voltage range. IEEE Trans. Power Electron. 33 (4), 3106–3114.

Kisacikoglu, M.C., Bedir, A., Ozpineci, B., Tolbert, L.M., 2012. Phev-EV charger technology assessment with an emphasis on V2g operation. Oak Ridge Nat. Lab., Oak Ridge, TN, USA, Tech. Rep. ORNL/TM-2010/221.

Kisacikoglu, M.C., Kesler, M., Tolbert, L.M., 2014. Single-phase on-board bidirectional PEV charger for V2G reactive power operation. IEEE Trans. Smart Grid 6 (2), 767–775.

Kwon, M., Choi, S., 2017. An electrolytic capacitorless bidirectional EV charger for V2G and V2H applications. IEEE Trans. Power Electron. 32 (9), 6792–6799. http://dx.doi.org/10.1109/TPEL.2016.2630711.

Lazar, J.F., Martinelli, R., 2001. Steady-state analysis of the LLC series resonant converter. In: APEC 2001. Sixteenth Annual IEEE Applied Power Electronics Conference and Exposition (Cat. No. 01CH37181), Vol. 2. IEEE, pp. 728–735.

Lee, B.-K., Kim, J.-P., Kim, S.-G., Lee, J.-Y., 2017. An isolated/bidirectional PWM resonant converter for V2G(H) EV on-board charger. IEEE Trans. Veh. Technol. 66 (9), 7741–7750. http://dx.doi.org/10.1109/TVT.2017.2678532.

Li, H., Bai, L., Zhang, Z., Wang, S., Tang, J., Ren, X., Li, J., 2018b. A 6.6kW SiC bidirectional on-board charger. In: 2018 IEEE Applied Power Electronics Conference and Exposition. APEC, pp. 1171–1178. http://dx.doi.org/10.1109/APEC.2018.8341164.

Li, Y., Han, M., Yang, Z., Li, G., 2021a. Coordinating flexible demand response and renewable uncertainties for scheduling of community integrated energy systems with an electric vehicle charging station: A bi-level approach. IEEE Trans. Sustain. Energy 12 (4), 2321–2331. http://dx.doi.org/10.1109/TSTE.2021.3090463.

Li, B., Li, Q., Lee, F.C., 2018a. A WBG based three phase 12.5 kW 500 kHz CLLC resonant converter with integrated PCB winding transformer. In: 2018 IEEE Applied Power Electronics Conference and Exposition. APEC, pp. 469–475. http://dx.doi.org/10.1109/APEC.2018.8341053.

Li, B., Li, Q., Lee, F.C., Liu, Z., Yang, Y., 2018c. A high-efficiency high-density wide-bandgap device-based bidirectional on-board charger. IEEE J. Emerg. Sel. Top. Power Electron. 6 (3), 1627–1636.

Li, G., Sun, Q., Boukhatem, L., Wu, J., Yang, J., 2019. Intelligent vehicle-to-vehicle charging navigation for mobile electric vehicles via VANET-based communication. IEEE Access 7, 170888–170906.

Li, H., Wang, S., Zhang, Z., Zhang, J., Li, M., Gu, Z., Ren, X., Chen, Q., 2021b. Bidirectional synchronous rectification on-line calculation control for high voltage applications in SiC bidirectional LLC portable chargers. IEEE Trans. Power Electron. 36 (5), 5557–5568. http://dx.doi.org/10.1109/TPEL.2020.3027703.

Li, Z., Xue, B., Wang, H., 2020a. An interleaved secondary-side modulated LLC resonant converter for wide output range applications. IEEE Trans. Ind. Electron. 67 (2), 1124–1135.

Li, H., Zhang, Z., Wang, S., Tang, J., Ren, X., Chen, Q., 2020b. A 300-kHz 6.6-kW SiC bidirectional LLC onboard charger. IEEE Trans. Ind. Electron. 67 (2), 1435–1445.

Liu, X., 2020. Dynamic response characteristics of fast charging station-EVs on interaction of multiple vehicles. IEEE Access 8, 42404–42421.

Liu, C., Wang, J., Colombage, K., Gould, C., Sen, B., 2016. A CLLC resonant converter based bidirectional EV charger with maximum efficiency tracking. In: 8th IET International Conference on Power Electronics, Machines and Drives. PEMD 2016, IET, pp. 1–6.

Lv, Z., Yan, X., Fang, Y., Sun, L., 2015. Mode analysis and optimum design of bidirectional CLLC resonant converter for high-frequency isolation of DC distribution systems. In: 2015 IEEE Energy Conversion Congress and Exposition. ECCE, IEEE, pp. 1513–1520.

Metwly, M.Y., Abdel-Majeed, M.S., Abdel-Khalik, A.S., Hamdy, R.A., Hamad, M.S., Ahmed, S., 2020. A review of integrated on-board EV battery chargers: Advanced topologies, recent developments and optimal selection of FSCW slot/pole combination. IEEE Access 8, 85216–85242.

Mohammed, S.A.Q., Jung, J.W., 2021. A comprehensive state-of-the-art review of wired/ wireless charging technologies for battery electric vehicles: Classification/common topologies/future research issues. IEEE Access 9, 19572–19585.

Mude, K.N., Aditya, K., 2019. Comprehensive review and analysis of two-element resonant compensation topologies for wireless inductive power transfer systems. Chinese J. Electr. Eng. 5 (2), 14–31.

Musavi, F., Craciun, M., Gautam, D.S., Eberle, W., Dunford, W.G., 2013a. An LLC resonant DC–DC converter for wide output voltage range battery charging applications. IEEE Trans. Power Electron. 28 (12), 5437–5445.

Musavi, F., Craciun, M., Gautam, D.S., Eberle, W., Dunford, W.G., 2013b. An LLC resonant DC–DC converter for wide output voltage range battery charging applications. IEEE Trans. Power Electron. 28 (12), 5437–5445.

Outeiro, M.T., Buja, G., Czarkowski, D., 2016. Resonant power converters: An overview with multiple elements in the resonant tank network. IEEE Ind. Electron. Mag. 10 (2), 21–45.

Pandey, R., Singh, B., 2019. A power-factor-corrected LLC resonant converter for electric vehicle charger using cuk converter. IEEE Trans. Ind. Appl. 55 (6), 6278–6286. http://dx.doi.org/10.1109/TIA.2019.2934059.

Pinto, J., Monteiro, V., Gonçalves, H., Afonso, J.a.L., 2013. Onboard reconfigurable battery charger for electric vehicles with traction-to-auxiliary mode. IEEE Trans. Veh. Technol. 63 (3), 1104–1116.

Pod-Point, Electric vehicle guides. URL https://pod-point.com/guides/vehicles?. (Accessed 05 Aug. 2021).

Salem, M., Jusoh, A., Idris, N.R.N., Das, H.S., Alhamrouni, I., 2018. Resonant power converters with respect to passive storage (LC) elements and control techniques–An overview. Renew. Sustain. Energy Rev. 91, 504–520.

Salem, M., Yahya, K., 2019. Resonant power converters. In: Electric Power Conversion. IntechOpen.

Severns, R., 1992. Topologies for three-element resonant converters. IEEE Trans. Power Electron. 7 (1), 89–98. http://dx.doi.org/10.1109/63.124581.

Shahzad, M.I., Iqbal, S., Taib, S., Masri, S., 2015. Design of a PEV battery charger with high power factor using half-bridge LLC-src operating at resonance frequency. In: 2015 IEEE International Conference on Control System, Computing and Engineering. ICCSCE, pp. 424–429. http://dx.doi.org/10.1109/ICCSCE.2015.7482223.

Shang, M., Wang, H., 2018. A voltage quadrupler rectifier based pulsewidth modulated LLC converter with wide output range. IEEE Trans. Ind. Appl. 54 (6), 6159–6168.

Shen, Y., Wang, H., Al-Durra, A., Qin, Z., Blaabjerg, F., 2019. A structure-reconfigurable series resonant DC–DC converter with wide-input and configurable-output voltages. IEEE Trans. Ind. Appl. 55 (2), 1752–1764.

Siebke, K., Schobre, T., Mallwitz, R., 2019. Comparison of GaN based CLLC converters for EV chargers operating at different switching frequency ranges. In: 2019 21st European Conference on Power Electronics and Applications. EPE '19 ECCE Europe, pp. P.1–P.9. http://dx.doi.org/10.23919/EPE.2019.8915565.

Steigerwald, R., 1988. A comparison of half-bridge resonant converter topologies. IEEE Trans. Power Electron. 3 (2), 174–182. http://dx.doi.org/10.1109/63.4347.

Tan, X., Ruan, X., 2016. Equivalence relations of resonant tanks: A new perspective for selection and design of resonant converters. IEEE Trans. Ind. Electron. 63 (4), 2111–2123.

Tanaka, T., Sekiya, T., Tanaka, H., Okamoto, M., Hiraki, E., 2013. Smart charger for electric vehicles with power-quality compensator on single-phase three-wire distribution feeders. IEEE Trans. Ind. Appl. 49 (6), 2628–2635.

Valente, M., Wijekoon, T., Freijedo, F., Pescetto, P., Pellegrino, G., Bojoi, R., 2021. Integrated on-board EV battery chargers: New perspectives and challenges for safety improvement. In: 2021 IEEE Workshop on Electrical Machines Design, Control and Diagnosis. WEMDCD. pp. 349–356.

Wang, H., 2015. A hybrid ZVS resonant converter with reduced circulating current and improved voltage regulation performance. In: 2015 IEEE Transportation Electrification Conference and Expo. ITEC. pp. 1–8.

Wang, H., Dusmez, S., Khaligh, A., 2013. Design and analysis of a full-bridge LLC-based PEV charger optimized for wide battery voltage range. IEEE Trans. Veh. Technol. 63 (4), 1603–1613.

Wang, H., Dusmez, S., Khaligh, A., 2014a. Maximum efficiency point tracking technique for LLC-based PEV chargers through variable DC link control. IEEE Trans. Ind. Electron. 61 (11), 6041–6049.

Wang, H., Dusmez, S., Khaligh, A., 2014b. A novel approach to design EV battery chargers using SEPIC PFC stage and optimal operating point tracking technique for LLC converter. In: 2014 IEEE Applied Power Electronics Conference and Exposition. APEC 2014, pp. 1683–1689. http://dx.doi.org/10.1109/APEC.2014.6803532.

Wang, H., Khaligh, A., 2013. Comprehensive topological analyses of isolated resonant converters in PEV battery charging applications. In: 2013 IEEE Transportation Electrification Conference and Expo. ITEC. pp. 1–7.

Wang, H., Li, Z., 2018. A PWM LLC type resonant converter adapted to wide output range in PEV charging applications. IEEE Trans. Power Electron. 33 (5), 3791–3801.

Wang, H., Shang, M., Shu, D., 2019. Design considerations of efficiency enhanced LLC pev charger using reconfigurable transformer. IEEE Trans. Veh. Technol. 68 (9), 8642–8651.

Williamson, S.S., Rathore, A.K., Musavi, F., 2015. Industrial electronics for electric transportation: Current state-of-the-art and future challenges. IEEE Trans. Ind. Electron. 62 (5), 3021–3032.

Wu, H., Li, Y., Xing, Y., 2016. LLC resonant converter with semiactive variable-structure rectifier (SA-VSR) for wide output voltage range application. IEEE Trans. Power Electron. 31 (5), 3389–3394.

Xuan, Y., Yang, X., Chen, W., Liu, T., Hao, X., 2021. A novel three-level CLLC resonant DC–DC converter for bidirectional EV charger in DC microgrids. IEEE Trans. Ind. Electron. 68 (3), 2334–2344. http://dx.doi.org/10.1109/TIE.2020.2972446.

Xue, B., Wang, H., Liang, J., Cao, Q., Li, Z., 2021. Phase-shift modulated interleaved LLC converter with ultrawide output voltage range. IEEE Trans. Power Electron. 36 (1), 493–503.

Yang, B., 2003. Topology Investigation of Front End DC/DC Converter for Distributed Power System (Ph.D. thesis). Virginia Tech.

Yang, D., Duan, B., Ding, W., Zhang, C., Song, J., Bai, H., 2020. Turn-off delay-controlled bidirectional DC–DC resonant converter with wide gain range and high efficiency. IEEE Trans. Transp. Electrif. 6 (1), 118–130. http://dx.doi.org/10.1109/TTE.2020.2965326.

Yang, B., Lee, F., Zhang, A., Huang, G., 2002. LLC resonant converter for front end DC/ DC conversion. In: APEC. Seventeenth Annual IEEE Applied Power Electronics Conference and Exposition (Cat. No.02CH37335), Vol. 2. pp. 1108–1112.

Yilmaz, M., Krein, P.T., 2013. Review of battery charger topologies, charging power levels, and infrastructure for plug-in electric and hybrid vehicles. IEEE Trans. Power Electron. 28 (5), 2151–2169.

Youssef, M.Z., Jain, P.K., 2004. A review and performance evaluation of control techniques in resonant converters. In: 30th Annual Conference of IEEE Industrial Electronics Society, Vol. 1. 2004. IECON 2004, IEEE, pp. 215–221.

Youssef, M., Jain, P.K., Zhang, H., 2005. Performance of the resonant converters under the self-sustained oscillation based control techniques. In: 2005 IEEE 36th Power Electronics Specialists Conference. IEEE, pp. 2750–2757.

Yuan, J., Dorn-Gomba, L., Callegaro, A.D., Reimers, J., Emadi, A., 2021. A review of bidirectional on-board chargers for electric vehicles. IEEE Access 9, 51501–51518. http://dx.doi.org/10.1109/ACCESS.2021.3069448.

Yuan, J., Dorn-Gomba, L., Callegaro, A.D., Reimers, J., Emadi, A., 2021. A review of bidirectional on-board chargers for electric vehicles. IEEE Access 9, 51501–51518.

Zeng, J., Zhang, G., Yu, S.S., Zhang, B., Zhang, Y., 2020. LLC resonant converter topologies and industrial applications—A review. Chinese J. Electr. Eng. 6 (3), 73–84.

Zhang, Z., Liu, C., Wang, M., Si, Y., Liu, Y., Lei, Q., 2020. High-efficiency high-power-density CLLC resonant converter with low-stray-capacitance and well-heat-dissipated planar transformer for EV on-board charger. IEEE Trans. Power Electron. 35 (10), 10831–10851.

Zou, S., Lu, J., Mallik, A., Khaligh, A., 2017a. 3.3 KW CLLC converter with synchronous rectification for plug-in electric vehicles. In: 2017 IEEE Industry Applications Society Annual Meeting. IEEE, pp. 1–6.

Zou, S., Lu, J., Mallik, A., Khaligh, A., 2017b. Bi-directional CLLC converter with synchronous rectification for plug-in electric vehicles. IEEE Trans. Ind. Appl. 54 (2), 998–1005.

Zou, S., Mallik, A., Lu, J., Khaligh, A., 2019. Sliding mode control scheme for a CLLC resonant converter. IEEE Trans. Power Electron. 34 (12), 12274–12284. http://dx.doi.org/10.1109/TPEL.2019.2904456.

Further reading

Pod-Point, EV charging solutions. URL https://new.abb.com/ev-charging. (Accessed 08 Aug. 2021).